Characterization of INCB086550: A Potent and Novel Small-Molecule PD-L1 Inhibitor

Holly K. Koblish, Liangxing Wu, Liang-Chuan S. Wang, Phillip C.C. Liu, Richard Wynn, Jonathan Rios-Doria, Susan Spitz, Hao Liu, Alla Volgina, Nina Zolotarjova, Kanishk Kapilashrami, Elham Behshad, Maryanne Covington, Yan-ou Yang, Jingwei Li, Sharon Diamond, Maxim Soloviev, Kevin O'Hayer, Stephen Rubin, Chrysi Kanellopoulou, Gengjie Yang, Mark Rupar, Darlise DiMatteo, Luping Lin, Christina Stevens, Yue Zhang, Pramod Thekkat, Ryan Geschwindt, Cindy Marando, Swamy Yeleswaram, Jeff Jackson, Peggy Scherle, Reid Huber, Wenqing Yao, and Gregory Hollis

Illustration by Bianca Dunn
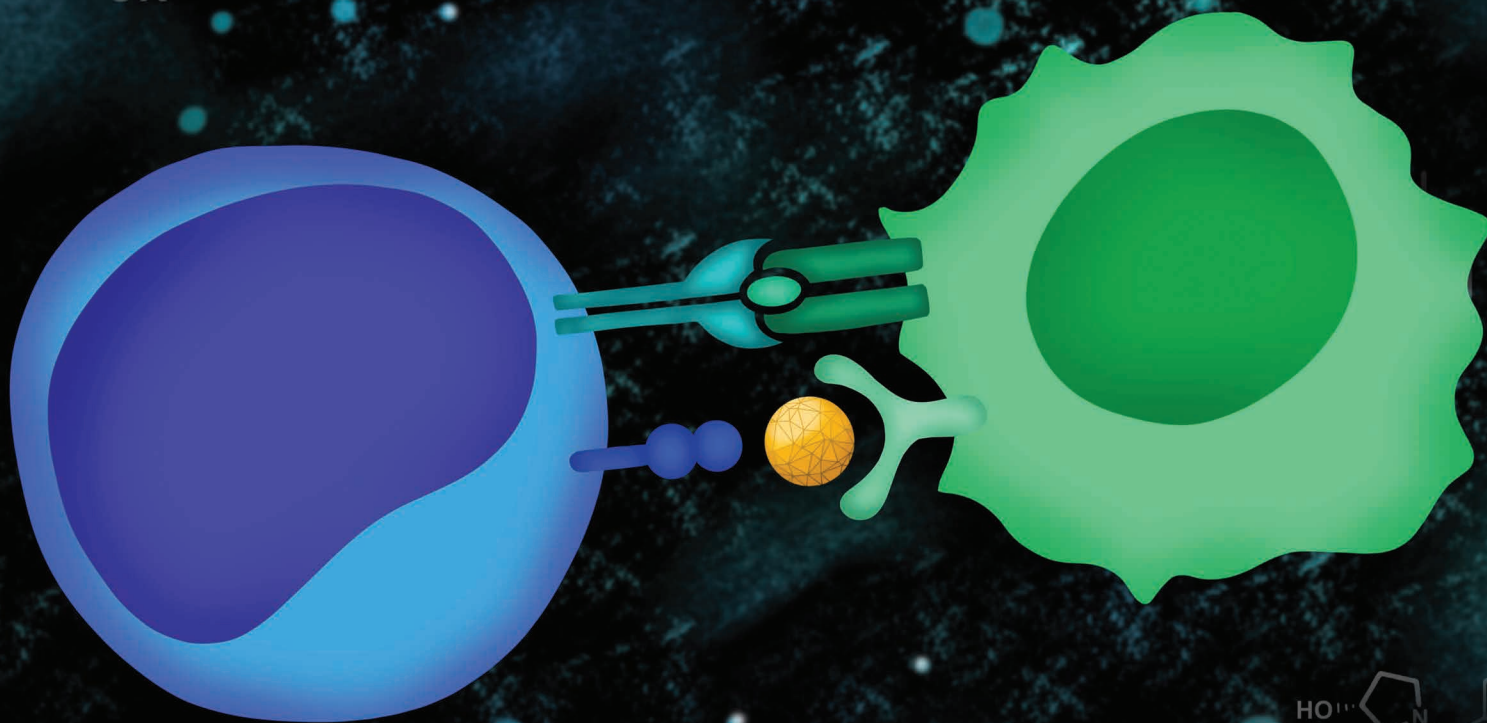
ABSTRACT

Blocking the activity of the programmed cell death protein 1 (PD-1) inhibitory receptor with therapeutic antibodies against either the ligand (PD-L1) or PD-1 itself has proven to be an effective treatment modality for multiple cancers. Contrasting with antibodies, small molecules could demonstrate increased tissue penetration, distinct pharmacology, and potentially enhanced antitumor activity. Here, we describe the identification and characterization of INCB086550, a novel, oral, small-molecule PD-L1 inhibitor. *In vitro*, INCB086550 selectively and potently blocked the PD-L1/PD-1 interaction, induced PD-L1 dimerization and internalization, and induced stimulation-dependent cytokine production in primary human immune cells. *In vivo*, INCB086550 reduced tumor growth in CD34+ humanized mice and induced T-cell activation gene signatures, consistent with PD-L1/PD-1 pathway blockade. Preliminary data from an ongoing phase I study confirmed PD-L1/PD-1 blockade in peripheral blood cells, with increased immune activation and tumor growth control. These data support continued clinical evaluation of INCB086550 as an alternative to antibody-based therapies.

SIGNIFICANCE: We have identified a potent small-molecule inhibitor of PD-L1, INCB086550, which has biological properties similar to PD-L1/PD-1 monoclonal antibodies and may represent an alternative to antibody therapy. Preliminary clinical data in patients demonstrated increased immune activation and tumor growth control, which support continued clinical evaluation of this approach.

See related commentary by Capparelli and Aplin, p. 1413.

INTRODUCTION

The immune system plays an important role in controlling and eradicating cancer; however, cancer cells often adopt mechanisms to evade or suppress the immune response that favor their growth. One mechanism involves altering the expression and function of costimulatory and coinhibitory molecules expressed on immune cells (1), key among which is the programmed cell death protein 1 (PD-1), which upon binding to its ligand (PD-L1) inhibits immune activation (2, 3). The centrality of the PD-L1/PD-1 axis indicates that pharmacologic intervention to disrupt this interaction would enable the immune system to control cancer; therapeutic antibodies against either PD-L1 or PD-1 that inhibit the PD-L1/PD-1 interaction have proven to be an effective treatment modality in multiple tumor types (2, 3), and several have gained FDA approval (2, 4, 5). This activity was modeled well preclinically, as blocking the PD-L1/PD-1 interaction with antibodies improves T-cell responses in a range of cancer models, induces cytokine production and cytolytic activity against tumor cells, and increases proliferation and infiltration of tumor-reactive CD8+ T cells into established tumors (6–9).
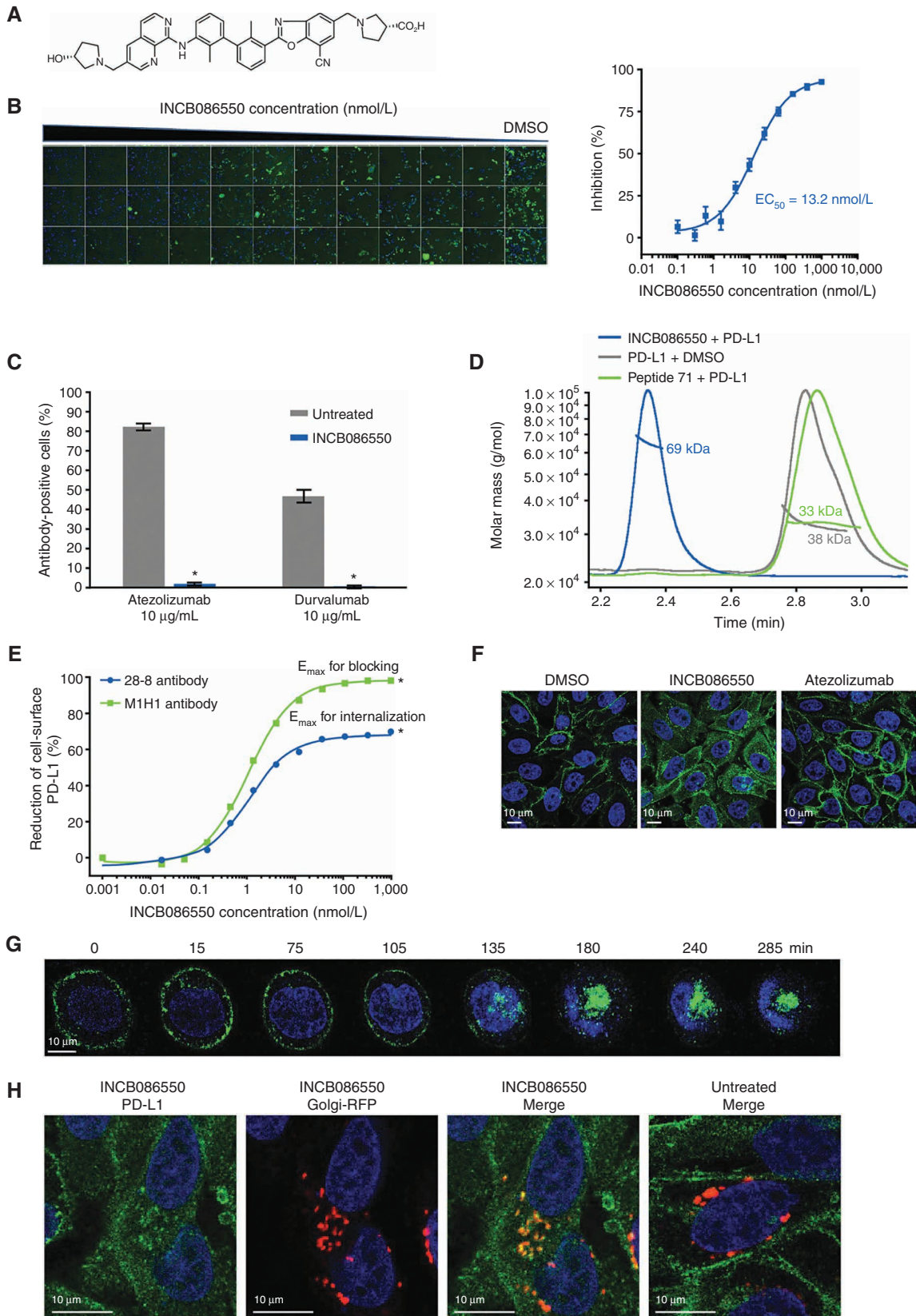
In contrast to therapeutic antibodies, small-molecule PD-L1/PD-1 inhibitors possess the important advantage of a shorter half-life, which may allow for dose titration and schedule modifications to minimize immune-related adverse events and maximize benefit/risk ratio. Oral administration also allows for more convenient dosing both as monotherapy and in combination with other molecularly targeted agents. Notably, these agents also often show increased tissue penetration and have potential for enhanced antitumor activity (10, 11).

Although early efforts identified small molecules capable of blocking the PD-1/PD-L1 interaction, well-characterized drug-like agents have not been previously reported (12). Herein, the novel small-molecule INCB086550 is described, which binds with high affinity to PD-L1, potently blocks the PD-L1/PD-1 interaction, and ablates ligand-induced signaling in disease-relevant cellular models. Mechanistically, INCB086550 induced dimerization and internalization of PD-L1, thereby removing the ability of the tumor cell to initiate the immunosuppressive action of the PD-1 pathway in T cells. Importantly, *in vivo*, INCB086550 reduced tumor growth in mice and induced T-cell activation gene signatures consistent with PD-L1/PD-1 pathway blockade. Moreover, PD-L1/PD-1 blockade by INCB086550 increased immune activation in whole blood samples from patients with advanced solid tumors enrolled in an ongoing phase I study of INCB086550; preliminary data identified tumor growth control in one patient (ClinicalTrials.gov identifier NCT03762447). These data highlight the potential for small-molecule PD-L1 antagonists as promising treatments for patients with cancer.

RESULTS

Discovery of a Small-Molecule Inhibitor of PD-L1

A rational medicinal chemistry approach led to the invention of INCB086550 (Fig. 1A). INCB086550 binding to

Incyte Research Institute, Wilmington, DE.

Corresponding Author: Jonathan Rios-Doria, Incyte Corporation, 1801 Augustine Cut Off, Wilmington, DE 19803. Phone: 302-498-6914; E-mail: jdoria@incyte.com

American Association for Cancer Research

recombinant human, mouse, rat, and cynomolgus PD-L1 was measured in a homogeneous time-resolved fluorescence (HTRF)–based PD-L1/PD-1 interaction assay. The half-maximal inhibitory concentration (IC_{50}) values for human, cynomolgus, and rat PD-L1 were 3.1, 4.9, and 1.9 nmol/L, respectively (Table 1). Binding to mouse PD-L1 was not detected and can be explained by the isoleucine present at residue 115 in mouse PD-L1 compared with methionine present in human, monkey, and rat PD-L1 (13). Consistent with the selectivity of INCB086550 for PD-L1, binding of PD-L2 to human PD-1 was not inhibited by INCB086550 at concentrations up to 10 μmol/L (Table 1). To determine whether INCB086550 could disrupt the PD-L1/PD-1 interaction on cells, imaging studies were performed using Chinese hamster ovary (CHO) cells expressing human PD-L1 (CHO PD-L1). INCB086550 inhibited binding of phycoerythrin (PE)-labeled PD-1 (PD-1/PE) to cell-surface PD-L1, with an IC_{50} of 13 nmol/L and >90% inhibition at concentrations ≥160 nmol/L (Fig. 1B). Flow cytometry demonstrated that pretreatment of CHO PD-L1 cells with INCB086550 blocked binding of the clinical anti–PD-L1 monoclonal antibodies (mAb) atezolizumab and durvalumab to PD-L1, suggesting that INCB086550 and the anti–PD-L1 mAbs compete for overlapping binding sites (Fig. 1C). Consistent with this, INCB086550 also inhibited binding of atezolizumab and durvalumab to PD-L1 in a surface plasmon resonance-based assay (Supplementary Fig. S1A and S1B). Taken together, INCB086550 potently and selectively binds to PD-L1 at a site that overlaps with the clinical anti–PD-L1 mAbs.

Investigation of the Mechanism of Action of INCB086550

The interaction of INCB086550 with PD-L1 was further characterized in biochemical and biophysical experiments. Size-exclusion chromatography with multiangle light scattering (SEC-MALS) was used to determine the molecular weight of PD-L1 in complex with INCB086550 or with the macrocyclic peptide, peptide 71 (14, 15), which binds human PD-L1 protein with an IC_{50} of 11.8 nmol/L. Elution of PD-L1 in the presence of dimethyl sulfoxide (DMSO) yielded a peak at 38 kDa, which is consistent with the molecular weight of monomeric PD-L1. In the presence of peptide 71, a peak at approximately 33 kDa was observed, confirming that the peptide binds PD-L1 in 1:1 stoichiometry and that PD-L1 remained monomeric in solution, as reported previously (16). In contrast, PD-L1 in the

Table 1. Biochemical and cellular potencies of INCB086550

Assay	Species	IC_{50}	n
Biochemical			
PD-L1			
	Human	3.1 ± 1.2 nmol/L	28
	Cynomolgus	4.9 ± 1.6 nmol/L	20
	Rat	1.9, <1.5 nmol/L	2
	Mouse	>10 μmol/L	
PD-L2	Human	>10 μmol/L	
Cellular			
SHP recruitment		6.3 ± 2.5 nmol/L	22
NFAT activation		21.4 ± 8.4 nmol/L	31

Abbreviations: NFAT, nuclear factor of activated T cells; SHP, SH2-domain-containing phosphatase.

presence of INCB086550 yielded a peak at ~69 kDa, indicating that INCB086550 binds PD-L1 in a 1:2 stoichiometry and induces PD-L1 dimerization (Fig. 1D). INCB086550-induced PD-L1 dimerization was also demonstrated by isothermal titration calorimetry (ITC), which showed a binding stoichiometry of 0.6, corresponding to the formation of a dimeric PD-L1:INCB086550 complex (Supplementary Fig. S1C). INCB086550-induced PD-L1 dimerization was further demonstrated in chemical cross-linking experiments using HCC827 cells (Supplementary Fig. S1D). In summary, these experiments confirmed PD-L1 dimer formation by INCB086550 but not by peptide 71 for both recombinant and cell surface–associated PD-L1.

Multiple antibodies were used to characterize the effect of INCB086550-induced binding and dimerization. First, the competition between INCB086550 and anti–PD-L1 antibodies described previously was confirmed using two mAbs against human PD-L1 on CHO PD-L1 and in MDA-MB-231 breast cancer cells, both of which express high levels of PD-L1. Anti–PD-L1 antibody clone MIH1 competed with INCB086550 for binding to CHO PD-L1 cells, whereas antibody clone 28-8 did not (Supplementary Fig. S1E). Thus, clone 28-8 binding evaluates the total amount of cell-surface PD-L1, and clone MIH1 binding reflects blockade of the epitope targeted by both the small-molecule and the clinical antibodies. To determine the effect of INCB086550 on epitope binding and total cell-surface PD-L1, CHO PD-L1 cells were treated with increasing concentrations of INCB086550 and stained with

Figure 1. INCB086550 binds to PD-L1 and interrupts its interaction with PD-1 and also induces PD-L1 dimerization and internalization. **A,** Structure of INCB086550. **B,** INCB086550 antagonizes binding of PD-1 to cells expressing PD-L1. CHO PD-L1 cells were treated with increasing concentrations of INCB086550, with each concentration run in triplicate. Each image is a composite of several fields of view within a single well. Nuclei stained with Hoechst 33342 and PD-1/PE were pseudocolored blue and green, respectively. The percent inhibition relative to the DMSO control is graphed. **C,** CHO PD-L1 cells were incubated with 1 μmol/L of INCB086550, followed by incubation with 10 μg/mL of atezolizumab or durvalumab. Binding of atezolizumab to cells was detected with anti-human IgG, conjugated to AlexaFluor488. Data were significant ($P < 0.05$) between untreated and 86550 pretreated for both atezolizumab and durvalumab by the Student t test. **D,** SEC-MALS reveals an inhibitor-induced dimeric PD-L1 complex. SEC-MALS profiles of either 15 μmol/L of PD-L1 alone (gray) or complexed with 100 μmol/L INCB086550 (blue). **E,** CHO PD-L1 cells were preincubated with increasing concentrations of INCB086550 for 18 hours, followed by staining with anti–PD-L1 clone MIH1 or 28-8. Percent inhibition was calculated based on the reduction of the fluorescent signal with the antibodies; $P < 0.05$ using Student t test. **F,** CHO PD-L1 cells were treated with 1 μmol/L of INCB086550 or atezolizumab at 10 μg/mL for 18 hours. After fixation, cells were stained with anti–PD-L1 clone 28-8 (green) and DAPI (blue). Scale bar, 10 μm. **G,** Live-cell imaging of CHO PD-L1 cells stained with PD-L1 (green) and DAPI (blue) and treated with INCB086550. Images up to 285 minutes are shown. Scale bar, 10 μm. **H,** CHO PD-L1 cells were transduced with a fusion construct of human Golgi-resident enzyme (N-acetylgalactosaminyltransferase) and TagRFP (red). Cells were then treated with INCB086550 at 1 μmol/L for 18 hours, fixed and stained with anti–PD-L1 antibody (green). Nuclei were visualized with DAPI (blue). Scale bar, 10 μm.

either clone MIH1 or 28-8. Flow cytometry using clone 28-8 showed approximately 70% reduction of PD-L1 staining, suggesting significant removal of PD-L1 from the cell surface. However, >90% epitope occupancy of PD-L1 and an IC_{50} of 1.1 nmol/L was determined using the MIH1 clone, confirming complete reduction in PD-L1 availability (Fig. 1E).

The observed decrease in cell-surface PD-L1 after treatment was confirmed using CHO PD-L1 cells treated with increasing concentrations of INCB086550 or atezolizumab. Immunoprecipitation experiments demonstrated that INCB086550, but not atezolizumab, reduced the amount of cell-surface PD-L1, supporting PD-L1 internalization (Supplementary Fig. S1F). Treatment of CHO PD-L1 cells with a close structural analogue of INCB086550 devoid of measurable PD-L1 binding (negative control) resulted in negligible changes in total PD-L1, whereas treatment with INCB086550 resulted in a decrease of overall PD-L1 in cells (Supplementary Fig. S1G). In confocal microscopy studies, clone 28-8 staining of cells treated with INCB086550 demonstrated internalization of PD-L1 and increased cytoplasmic staining (green, Fig. 1F) in CHO PD-L1 cells, whereas atezolizumab induced only minor levels of PD-L1 internalization, consistent with published reports (17). Live-cell imaging demonstrated rapid internalization of PD-L1 following INCB086550 treatment that appeared maximal ~4 hours after treatment (Fig. 1G; Supplementary Video). Additional experiments showed colocalization of internalized receptor with Golgi-specific staining, suggesting endosome-to-Golgi receptor transport. Thus, unlike the PD-L1 antibody atezolizumab, INCB086550 induced PD-L1 entry into Golgi vesicles, leading to subsequent trafficking to the nucleus (Fig. 1H). These data are consistent with previous reports of translocation of PD-L1 from plasma membrane to nucleus through endocytic pathway (18). Overall, INCB086550 induces the dimerization of cell-surface PD-L1, resulting in internalization.

INCB086550 Functions in Cells to Block PD-1–Mediated Signaling and Stimulate Cellular Immune Activation

The relationship between the potency of INCB086550 for inducing PD-L1 dimerization and internalization and the level of cell-surface expression of PD-L1 was assessed using isogenic cells derived from the mouse bladder tumor line-2 (MBT2), which was developed by deleting mouse PD-L1 and expressing human PD-L1. Three MBT2 clones with low, medium, and high levels of human PD-L1, respectively, were selected to test relative potencies of INCB086550-mediated PD-L1 internalization using the MIH1 antibody. The half-maximal effective concentration (EC_{50}) values of 3.7 nmol/L (MBT2-PD-L1 low), 0.4 nmol/L (MBT2-PD-L1 medium), and 0.1 nmol/L (MBT2-PD-L1 high) inversely correlated with PD-L1 expression (Fig. 2A). The EC_{50} curve for PD-L1 low clone was significantly different from PD-L1 medium and high clones ($P < 0.05$). Similar data were obtained using pleural effusion macrophages from a patient with non–small cell lung cancer. The EC_{50} for the reduction in unoccupied cell-surface PD-L1 was 21 nmol/L when tested in control cultures but decreased to 4.7 nmol/L when the cells were pretreated with interferon gamma (IFNγ), which increased PD-L1 levels approximately 5-fold, suggesting that ligand density drives

potency (Fig. 2B). The kinetics of restoration of unoccupied cell-surface PD-L1 were investigated in MDA-MB-231 cells by treating with INCB086550 for 20 hours, washing to remove compound, and staining cells with anti–PD-L1 clone MIH1 at various time points. Unoccupied cell-surface PD-L1 was restored to nearly 50% of baseline levels within 48 hours and was almost completely restored to baseline 120 hours after INCB086550 was removed (Fig. 2C).

Additionally, the potency of INCB086550 for reducing unoccupied cell-surface PD-L1 was determined in monocytes from multiple species in whole blood. Resulting EC_{50} values of 4.5 and 88 nmol/L for cynomolgus monkey and human, respectively (Fig. 2D), indicated that the cynomolgus monkey was a pharmacologically relevant toxicology species during our drug-discovery program and that this assay could be used to measure activity during our clinical evaluation of INCB086550.

The functional outcome of disrupting the PD-L1/PD-1 interaction with INCB086550 was assessed in cell-based assays. Ligation of PD-1 with PD-L1 recruits SH2 domain-containing phosphatase (SHP) 1/2 to inhibit T-cell receptor signaling and to attenuate activation of the nuclear factor of activated T cells (NFAT) pathway (19). Our results show that INCB086550 potently ablates PD-1–mediated SHP recruitment (IC_{50} = 6.3 nmol/L) and enhances NFAT signaling (EC_{50} = 21.4 nmol/L; Table 1). T-cell function was also evaluated in cytokine secretion assays performed with primary human cells. In the first assay, CHO cells engineered to express PD-L1 and an anti-CD3 single-chain antibody were incubated with human T cells in the presence of increasing concentrations of INCB086550. Analysis of cell supernatants demonstrated that INCB086550 treatment induced secretion of IFNγ in a concentration-dependent manner, with an EC_{50} of 9.8 nmol/L (Fig. 2E), and maximal levels of IFNγ were similar to those induced by atezolizumab (425% vs. 433% induction, respectively). In a second assay, blood from healthy human donors was pretreated with increasing concentrations of INCB086550 followed by the addition of staphylococcal enterotoxin B (SEB), and analysis of cell supernatants showed that INCB086550 treatment induced IFNγ production (Fig. 2F). These data demonstrate that INCB086550 depletes cell-surface PD-L1 more potently in cells with higher levels of PD-L1, and that this occurs across species. The data also show that INCB086550-induced PD-L1 depletion stimulates proinflammatory cytokine production in primary human immune cells, the maximum levels of which were similar to those induced by a clinically approved PD-L1 antibody. No overt toxicity to cells was observed with INCB086550 administration.

INCB086550 Distributes Well to Tumors Regardless of PD-L1 Levels

To understand the tumor distribution of INCB086550, pharmacokinetic/pharmacodynamic studies were performed in MDA-MB-231 tumor-bearing mice. Significant reductions of unoccupied cell-surface PD-L1 were seen on MDA-MB-231 tumors 24 hours after the first dose (Fig. 3A). This was dependent on the number of doses and the dose level, with reductions ranging from 26% to 91% relative to tumors from mice receiving control treatment. In the same model, greater than 50% inhibition of unoccupied
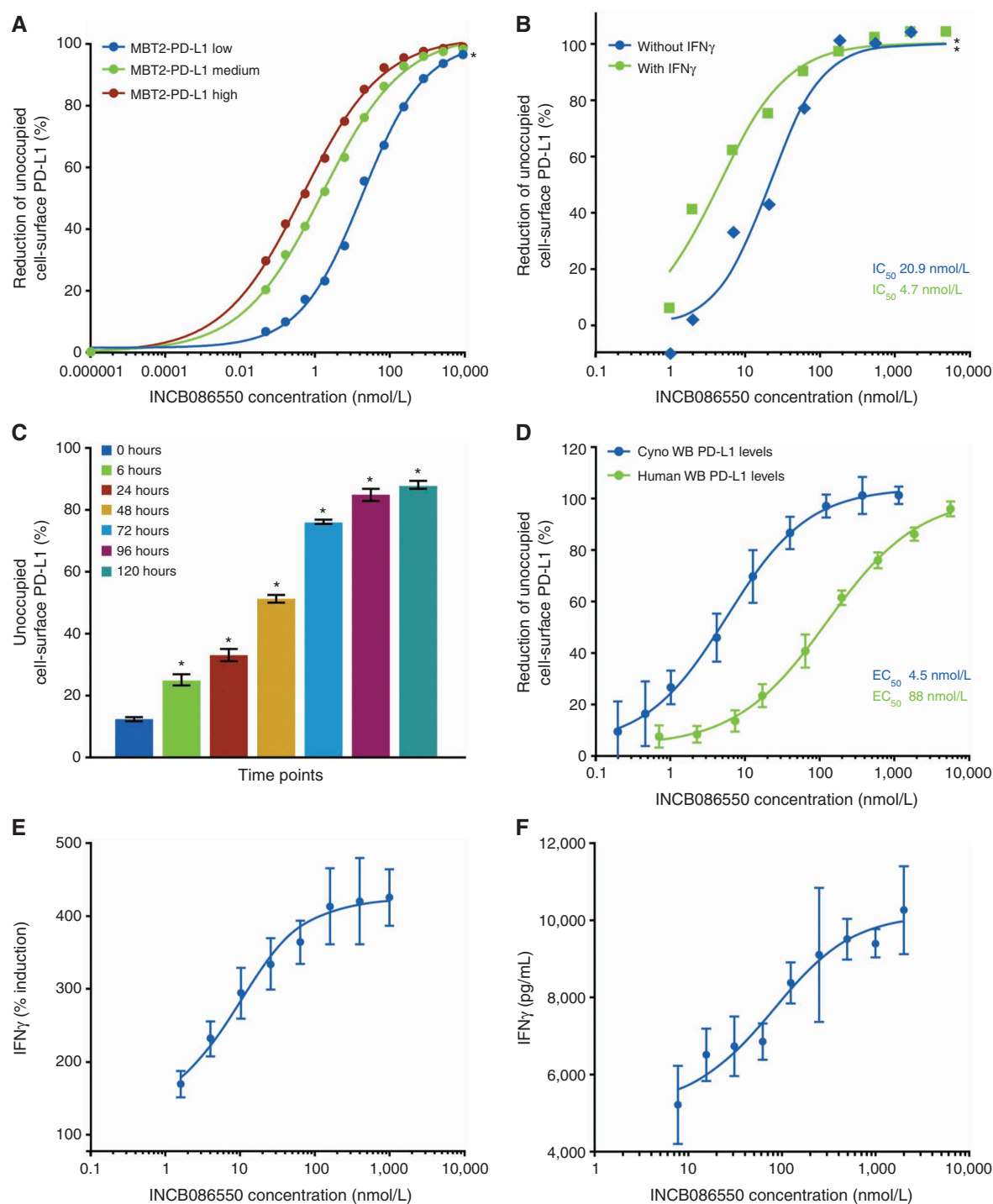
Figure 2. INCB086550 reduces available surface PD-L1 in various cell types and enhances T-cell activity. **A,** Isogenic MBT2 clones expressing different levels of PD-L1 were treated with various concentrations of INCB086550 for 16 hours. At the end of incubation, cells were harvested and stained for available surface human PD-L1, followed by flow-cytometric analysis. $P < 0.05$ for PD-L1–low clone as compared with PD-L1 medium and high clones by one-way ANOVA. **B,** Cells from pleural effusion fluids were left unstimulated or stimulated with 1 ng/mL of human IFNγ in the presence of various concentrations of INCB086550 for 20 hours. After the incubation, cells were stained and analyzed by flow-cytometric analysis. $P < 0.05$ by paired t test. **C,** MDA-MB-231 cells were treated with 250 nmol/L of INCB086550 for 18 hours. Residual compound was then removed with acid wash and cells were harvested at designated time points to determine levels of available PD-L1. Samples were run in triplicates, and the percentage of surface receptor was calculated using mean fluorescence intensity. Data were significant compared with time zero using one-way ANOVA with Dunnett multiple comparisons. **D,** Cynomolgus monkey and human whole blood was treated with INCB086550 and then stimulated with IFNγ for 20 hours. Cells were stained with anti–PD-L1 and anti-CD14 and flow-cytometric analysis was performed. **E,** T cells from normal human donors were mixed with CHO PD-L1 cells and treated with increasing concentrations of INCB086550 or atezolizumab at 10 nmol/L for 3 days. Human IFNγ levels were measured by Luminex. **F,** INCB086550 or atezolizumab was added to whole blood from normal human donors together with staphylococcal enterotoxin B and incubated for 5 days. IFNγ levels were measured by Luminex.
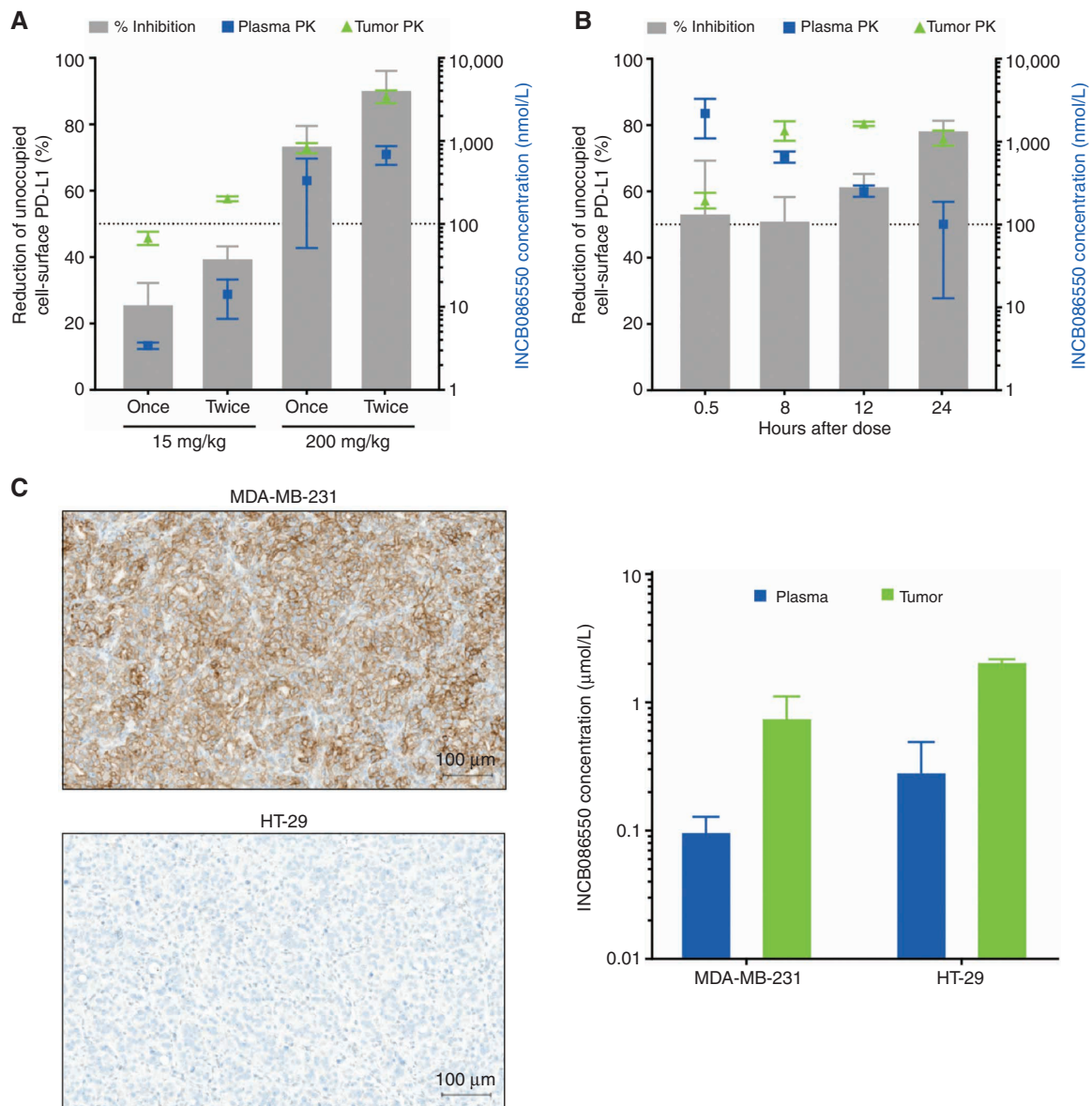
Figure 3. INCB086550 reduces tumor PD-L1 after *in vivo* administration. **A,** BALB/c nu/nu mice bearing MDA-MB-231 xenograft were treated orally with 15 or 200 mg/kg of INCB086550 once or twice with a 12-hour interval. Tumor samples were harvested at 24 hours after initial dose administration and processed into single-cell suspension to determine tumor PD-L1 expression by flow-cytometric analysis. Plasma samples were collected at 24 hours after initial dose administration to determine compound concentration by high-performance liquid chromatography (HPLC) assay. **B,** BALB/c nu/nu mice bearing MDA-MB-231 xenograft were dosed once with INCB086550 at 150 mg/kg. Plasma and tumor samples were collected at various time points to determine compound concentration by HPLC assay. Tumor samples were also processed into single-cell suspension to determine tumor PD-L1 expression by flow-cytometric analysis. **C,** MDA-MB-231 and HT-29 tumors engrafted in CD34+ humanized mice were analyzed for PD-L1 expression by IHC. MDA-MB-231 tumors were found to express abundant PD-L1. In contrast, HT-29 tumors were PD-L1–negative. Scale bar, 100 μm. MDA-MB-231 or HT-29 tumor–bearing humanized mice were dosed for 14 and 7 days, respectively, with 20 mg/kg INCB086550 twice daily. Plasma and tumor were collected 16 hours after the last dose and compound levels were analyzed.

cell-surface PD-L1 could be seen as early as 30 minutes after INCB086550 dosing; this increased to 78% inhibition at 24 hours as tumor levels of compound increased relative to plasma levels (Fig. 3B). Tumor penetration was not completely dependent on the dimerization and internalization of the compound with PD-L1, as INCB086550 was observed in the PD-L1–negative HT-29 tumors (Fig. 3C). Taken together, these data suggest a high tumor:plasma ratio for INCB086550 and the feasibility to inhibit greater

than 90% of unoccupied cell-surface PD-L1 for 24 hours in mice with twice daily (b.i.d.) dosing.

Immune-Mediated Mechanism of INCB086550 in Tumors

As it was shown above that INCB086550 does not bind to mouse PD-L1, humanized murine cancer models were utilized to assess the *in vivo* activity of INCB086550. Initially, MC38 tumors with a deletion of mouse PD-L1 and overexpression of

human PD-L1 (huPD-L1; ref. 17) were investigated. C57BL/6 mice with established MC38 huPD-L1 tumors were dosed orally b.i.d. with INCB086550. Robust and statistically significant antitumor efficacy was observed in immunocompetent mice, with tumor growth inhibition (TGI) of 32%, 66%, and 69% for 2, 20, and 200 mg/kg, respectively, on day 16 (Fig. 4A; $P < 0.05$ for 20 and 200 mg/kg). This activity was abolished when the same tumors were hosted in immunodeficient mice, consistent with an immune-mediated mechanism of action (Fig. 4B). The antitumor activity of INCB086550 was not significantly different from that of atezolizumab (73% TGI; $P > 0.05$; Fig. 4A). The effect of INCB086550 on PD-L1 levels in MC38 huPD-L1 tumors was assessed in mice receiving two doses of the compound. INCB086550 induced a dose-dependent decrease of PD-L1 available to bind to PD-1 using antibody clone MIH1 (Fig. 4C). Maximum reduction of occupied PD-L1 was >90% at the 200 mg/kg dose, which is consistent with the inhibition observed in the MDA-MB-231 model. Total cell-surface PD-L1 was also decreased, as measured using the 28-8 clone, which reflects internalized PD-L1. This degree of inhibition was associated with increased infiltrates of CD8+ T cells into the tumors (Fig. 4D). Therefore, these data demonstrate that, in the MC38 huPD-L1 model, binding of INCB086550 to PD-L1 reduces cell-surface PD-L1 availability, induces cytotoxic T-cell infiltration, and inhibits tumor growth.

To assess the activity of INCB086550 in a human tumor, CD34+ stem cell–engrafted humanized mice bearing MDA-MB-231 tumors were evaluated (20). Cell-surface PD-L1 is critical to growth in this humanized mouse model, as cells made deficient for PD-L1 do not grow past minimal engraftment (Supplementary Fig. S2). Dosing of mice with INCB086550 b.i.d. at 20, 60, or 200 mg/kg, or atezolizumab at 5 mg/kg twice weekly, resulted in TGIs of 55%, 54%, and 61%, respectively, which are comparable to the efficacy of atezolizumab (Fig. 4E) and the growth of the PD-L1–deficient line (Supplementary Fig. S2). Consistent with the findings in the MC38-huPD-L1 model, the activity of INCB086550 was abolished in MDA-MB-231 tumor-bearing immunodeficient mice, demonstrating that the activity is dependent on human CD34+ stem cell engraftment (Fig. 4F). INCB086550 levels in the plasma and tumors of treated mice at the end of the study were found to be similar to levels in short-term studies; tumor:plasma area under the curve ratios ranged from 5 to 10 across the dose groups (Fig. 4G). Importantly, all doses resulted in INCB086550 tumor concentrations greater than the whole blood IC$_{90}$ at trough (792 nmol/L). These data suggest that tumor PD-L1 is a target of INCB086550 in the humanized MDA-MB-231 tumor model.

To further understand the mechanism of action of INCB086550, MDA-MB-231 tumors from CD34+ humanized mice were treated with vehicle or INCB086550 at 20 mg/kg and subjected to RNA-sequencing (RNA-seq) analysis. Expression of genes known to be induced by the anti–PD-1 mAb nivolumab in melanoma tumors was analyzed (21). A 58-gene signature was identified from this published data set based on a log$_2$ fold-change cutoff of 1.2 and a P value of <0.05, and this was used to evaluate gene expression in tumors from INCB086550-treated mice. This gene signature in the INCB086550-treated tumors included increases in *Ifng*, *Pdcd1*, *Lag3*, and *Gzmb*, which is indicative of T-cell

activation. Most mice treated with vehicle had low expression of this gene set (Fig. 4H). Analysis of two of the three mice that had received INCB086550 had significant increases in the majority of genes within this gene set, including *LAG3*, *IFNG*, *IRF1*, *GZMA*, *GZMB*, and *GZMH*. Gene Ontology (GO) term enrichment analysis was performed, and the top GO terms for genes presented in Fig. 4H were immune response, lymphocyte activation, and positive regulation of programmed cell death. Gene-expression changes for each individual gene are shown in Supplementary Fig. S3 and Supplementary Table S1. These data show that INCB086550 selectively induces IFNγ-related genes consistent with T-cell activation as the primary mechanism of action for antitumor activity, which resembles observations made in patients receiving checkpoint blockade therapy.

Importantly, INCB086550 demonstrated no adverse effects in mice, and in the pivotal 28-day toxicology studies in rats and monkeys, INCB086550 was well tolerated at all tested doses up to 1,000 mg/kg. Events associated with INCB086550 in rats were observed only at 1,000 mg/kg/day and included decreased red blood cell mass (red blood cells, hemoglobin, and hematocrit), higher reticulocyte counts and red cell distribution, higher neutrophil and monocyte counts, and histiocytic infiltrates in the duodenum, jejunum, and/or ileum, with increased apoptosis/necrosis in the ileum in both males and females. The severity of these events was minimal to mild, and they were thus considered nonadverse. Treatment-related events in monkeys were limited to emesis at doses ≥200 mg/kg/day, with no evidence of target organ toxicity.

INCB086550 Binds to PD-L1 and Elicits Immune Activation in Patients with Cancer

In an ongoing phase I study, pharmacodynamic markers of activity, including the binding of INCB086550 to PD-L1, measurement of downstream markers of the IFNγ pathway, and levels of cell-free PD-L1, were evaluated (22). After stimulation of whole blood samples with exogenous IFNγ, the average reduction of unoccupied cell-surface PD-L1 on monocytes was determined for increasing doses of INCB086550 over the dosing interval (0–8 hours) and at steady state (cycle 1 day 15) by flow cytometry using clone MIH1. After INCB086550 treatment, the *ex vivo* stimulation of whole blood showed a dose-dependent reduction in free PD-L1 on cells and reached maximum inhibition at 200 mg b.i.d. (Fig. 5A). The percent reduction compared with the predose PD-L1 baseline level was also dose dependent, reaching maximum inhibition at 200 mg b.i.d. and mirroring the pharmacokinetic measurement (Fig. 5A).

Downstream markers in the IFNγ pathway, CXCL9 and CXCL10, were measured in plasma samples from patients treated with INCB086550 in the clinical trial. CXCL9 [or monokine induced by gamma interferon (MIG)] is induced by IFNγ, but not by IFNα/β, and predominantly mediates lymphocytic infiltration to focal sites and suppresses tumor growth (23). CXCL10 [or IFNγ-induced protein 10 (IP-10)] is strongly induced by IFNγ and IFNα/β and plays a role in chemotaxis, apoptosis, cell growth, and angiogenesis (24). INCB086550 treatment elicited significant 1.8- and 1.4-fold increases in CXCL9 and CXCL10, respectively, at cycle 2 day 1, and a significant 3.8-fold increase in IFNγ at cycle 1 day 8,
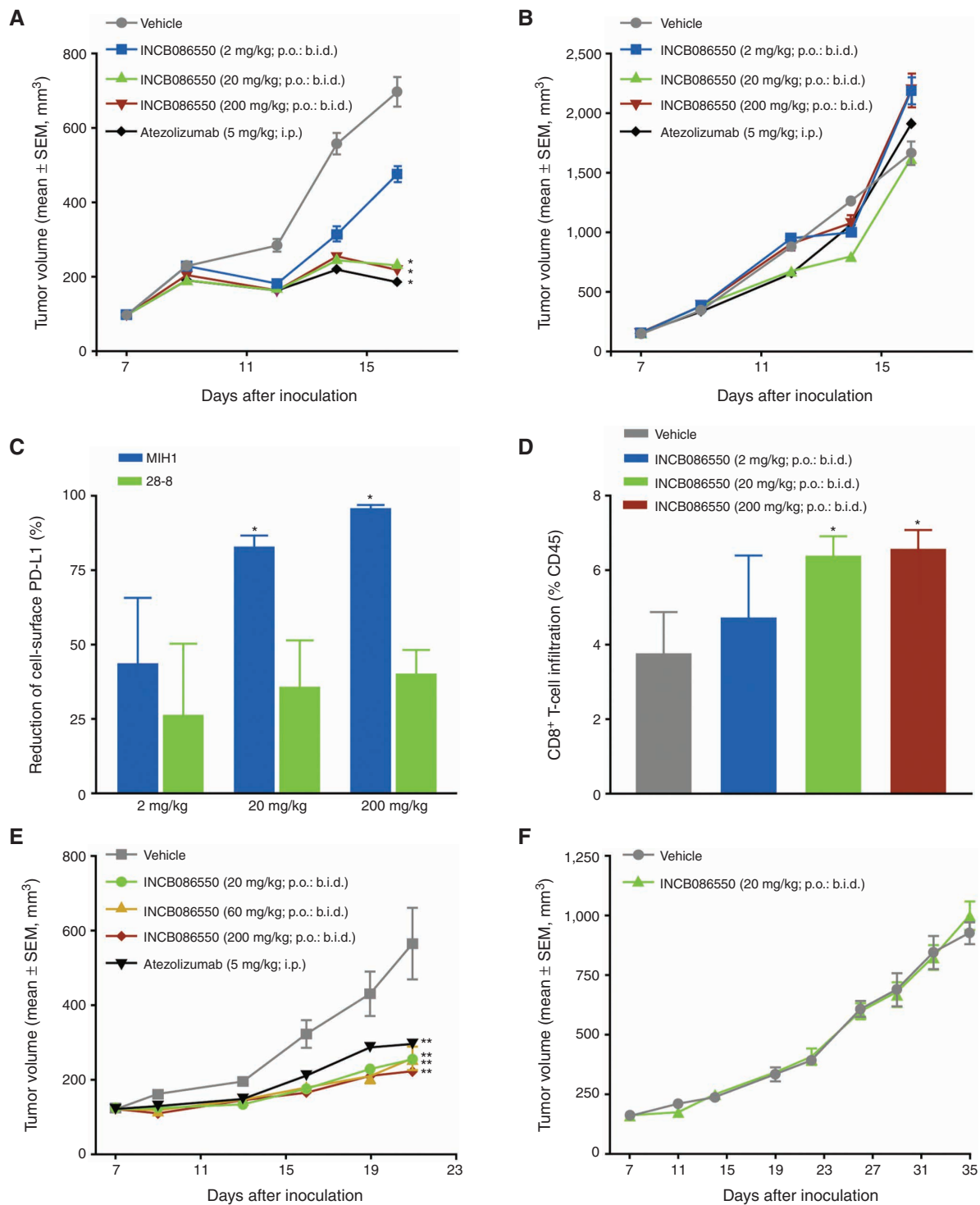
Figure 4. INCB086550 inhibits tumor growth in preclinical mouse models by reducing unoccupied cell-surface PD-L1 and increasing T-cell number and activation. Activity of orally dosed (p.o.) INCB086550 (2, 20, and 200 mg/kg b.i.d.) in C57BL/6 (**A**) or NSG (**B**) mice bearing established MC38-huPD-L1 tumors. **C,** Levels of unoccupied and occupied cell-surface PD-L1 on MC38-huPD-L1 tumors after dosing mice with INCB086550. $P < 0.05$ using Student t test. **D,** Percentage of intratumoral CD8+ T cells in MC38-huPD-L1 tumors at the end of the efficacy study measured by flow-cytometric analysis. $P < 0.05$ when compared with vehicle using one-way ANOVA. Activity of orally dosed INCB086550 in human CD34+ engrafted NSG (20, 60, and 200 mg/kg b.i.d.; **E**) or NSG (20 mg/kg; **F**) mice bearing established MDA-MB-231 tumors. Atezolizumab was included as a control at 5 mg/kg every 5 days in **E**. (*continued on following page*)
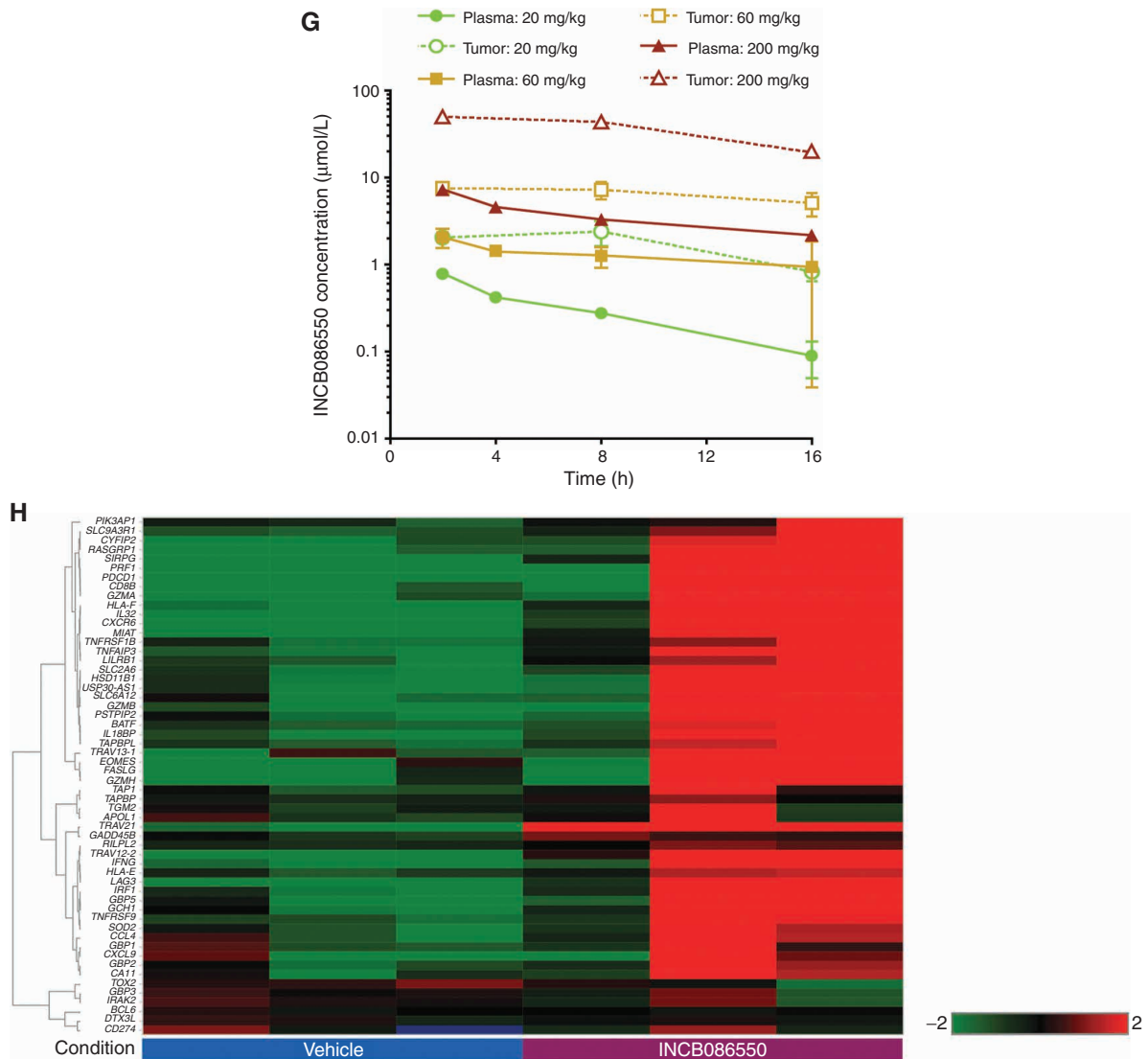
Figure 4. *(Continued)* **G,** At the end of the efficacy study in **E**, levels of INCB086550 were measured in plasma and tumors were collected, 2, 4, 8, and 16 hours after the last dose. **H,** MDA-MB-231 xenograft-engrafted CD34+ humanized NSG mice were orally administered INCB086550 at 20 mg/kg b.i.d. for 31 days. Tumors from humanized mice from one donor were collected at the end of the study for RNA-seq analysis. The heat map displays a signature of 58 genes that increased by at least 1.2-fold with $P < 0.05$ in tumors from patients with melanoma who received nivolumab.

compared with baseline (Fig. 5B–D). Increases were observed at doses greater than 200 mg every day. A statistically significant, dose-dependent 1.4-fold increase in the plasma concentration of cell-free PD-L1 was also observed across all dose levels at cycle 2 day 1 compared with baseline in the plasma of the patients in the clinical trial (ref. 22; Fig. 5E). Increases in the markers of immune activation and soluble PD-L1 were generally higher at higher doses.

On-treatment increases in plasma concentrations of CXCL10, and cell-free PD-L1, were confirmed by an Olink Proteomics proximity extension assay along with increases in other IFN-related cytokines and immune regulatory proteins including granzymes B and H (Fig. 5F). GO term enrichment analysis was performed, and the top GO terms for genes presented in Fig. 5F were regulation of leukocyte differentiation and regulation of adaptive immune response. In addition to

the dose-dependent pharmacodynamic effects, preliminary clinical activity of INCB086550 was observed in a 54-year-old female patient as a decrease in target lesion volume at week 24 of INCB086550 therapy (Fig. 5G).

Taken together, the assessments from the clinical study indicate that oral administration of INCB086550 provides dose-related pharmacodynamic immune activation similar to that reported for PD-L1 or PD-1 therapeutic antibodies and provides evidence that INCB086550 is biologically active in blocking PD-L1/PD-1 interactions, leading to T-cell activation.

DISCUSSION

Blocking the PD-L1/PD-1 checkpoint is an important mechanism to restoring T-cell effector function and
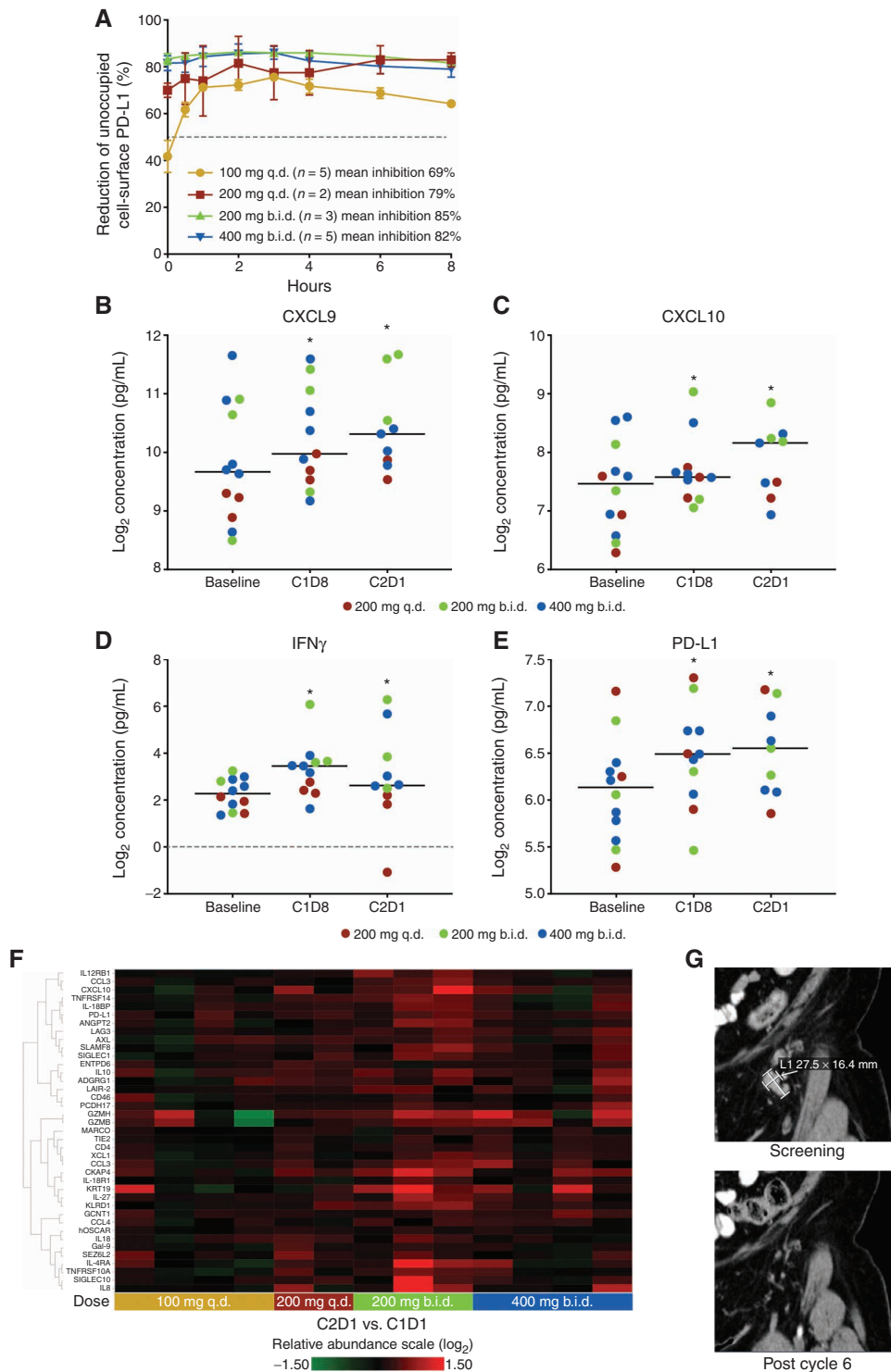
Figure 5. PD-L1 engagement, immune activation, and tumor volume reduction observed in patients with cancer in a phase I trial of INCB086550.
A, Dose-related decrease of free PD-L1 receptors in patient whole blood. The binding activity to PD-L1 on human blood monocytes was monitored in whole blood stimulated with exogenous IFNγ followed by the analysis of expression of PD-L1 by flow cytometry. Plasma samples were assessed on a targeted panel by immunoassay and on a panel of 1,104 analytes utilizing the Olink proximity extension assay platform. q.d., every day. On-treatment increases in CXCL9 (**B**), CXCL10 (**C**), IFNγ (**D**), and PD-L1 (**E**) were observed at cycle 1 day 8 and cycle 2 day 1 by immunoassay and confirmed by the Olink platform. **F,** Posttreatment increases in plasma concentrations of interferon-related cytokines and immune regulatory proteins including GZMH and GZMB were observed by the Olink platform. **G,** Clinical activity observed with INCB086550 in a 54-year-old female. Decrease in target lesion volume shown by CT scan at week 24 of INCB086550 therapy. Figure reproduced from Piha-Paul S, et al. Pharmacodynamic biomarkers demonstrate T-cell activation in patients treated with the oral PD-L1 inhibitor INCB086550 in a phase 1 clinical trial. Journal for ImmunoTherapy of Cancer 2020;8:doi: 10.1136/jitc-2020-SITC2020.0419 under the creative commons license (CC BY 4.0). Poster presented at SITC 2020.

antitumoral immunity (25). Monoclonal antibodies targeting either PD-L1 or PD-1 to disrupt T-cell inhibitory signaling have shown remarkable success in the clinic against a variety of cancers either as monotherapy or in combination with other antitumor agents. However, therapeutic PD-L1 or PD-1 mAbs have drawbacks including limited or no response in a large percentage of patients, possibly because of poor distribution to tumors and extended recovery times for patients experiencing immune-related adverse events (26, 27). Also, as with other antibody treatments, a clinic visit is required for intravenous dosing. A small molecule capable of inhibiting the PD-L1/PD-1 interaction may possess advantages over therapeutic mAbs, including oral bioavailability, increased tumor penetration, alternative safety profiles and a lack of antidrug antibodies (28). Herein, the preclinical and clinical activity of INCB086550, a novel small molecule able to potently disrupt the PD-L1/PD-1 interaction, has been described.

The results demonstrate that INCB086550 is a highly potent ligand for PD-L1 and prevents binding of PD-L1 to PD-1. It is selective for PD-L1 over PD-L2 and, owing to the single amino acid change at residue 115, interacts with human, cynomolgus, and rat but not mouse PD-L1 (13). Biophysical studies using ITC, SEC-MALS, and *in vitro* cross-linking show PD-L1 in a dimeric form in the presence of INCB086550. These data are consistent with other small molecules targeting this interaction (29). The mechanism of action for this molecule is 2-fold: it induces partial internalization of PD-L1 dimers and also blocks the interaction between PD-1 and the PD-L1 remaining on the cell surface. Therefore, although a portion of PD-L1 is internalized after INCB086550 treatment, the PD-L1 that is remaining at the cell surface is bound by compound and unable to bind to PD-1, providing maximal inhibition similar to mAbs. The observation that the extent of PD-L1 internalization was correlated with PD-L1 cell-surface expression reinforces the concept that internalization is dependent on dimerization occurring first, so that the higher levels of PD-L1 expression lead to more dimer formation and therefore more internalization. Because one of the mechanisms of tumor escape from immunosurveillance is upregulation of PD-L1 (3, 30, 31), this could be another reason to believe that small molecules with this mechanism may be particularly active in patients with tumors that have high expression of the ligand.

From a molecular pharmacologic standpoint, INCB086550 effectively restored NFAT pathway activation and abolished SHP recruitment to PD-1, thereby demonstrating functional inhibition of the PD-L1/PD-1 signaling pathway. INCB086550 dose-dependently reduced unoccupied cell-surface PD-L1 on the tumor cell surface *in vivo*, effectively inhibited tumor growth as a single agent in multiple humanized tumor models, and was well tolerated. Efficacy in preclinical models was equivalent to atezolizumab, which was consistent with *in vitro* functional studies showing similar maximal levels of IFNγ induction by atezolizumab and INCB086550 in primary human immune cells. Furthermore, RNA-seq analysis of tumors in CD34+ humanized mice demonstrated that INCB086550 increased gene expression of T-cell activation and IFN-responsive genes in tumors. These genes largely overlapped with genes known to be increased in patients who received the clinical PD-1 antibodies pembrolizumab

or nivolumab (21, 32). These data demonstrate that INCB086550 can generate similar gene-expression profiles as therapeutic PD-1 antibodies and validate the utility of preclinical CD34+ humanized mouse models to interrogate pharmacologic activity of immunotherapies (20).

Significant PD-L1 engagement and immune activation was observed in patients with cancer enrolled in an ongoing phase I trial, and tumor reduction is described for one of these patients. The binding activity to PD-L1 on human blood monocytes was dose dependent, mirrored the pharmacokinetic measurement, and reached maximum inhibition at 200 mg b.i.d. A dose-related increase in the plasma concentration of cell-free PD-L1 was observed, suggesting the expansion of tumor volume due to immune cell infiltration and lysis of the tumor (33). Furthermore, the targeted analysis of downstream markers in the IFNγ pathway, CXCL9 and CXCL10, measured in the plasma from patients treated with INCB086550, was increased after INCB086550 treatment, suggesting T-cell activation. Additionally, increases in proteins not included in the targeted assessment (such as granzymes B and H) were also observed. Therefore, the immune activation profile resulting from INCB086550 administration is qualitatively similar to that reported for PD-1 or PD-L1 therapeutic antibodies (34, 35). Furthermore, a decrease in tumor volume was observed in a patient showing emerging clinical activity.

Although the present results demonstrate that INCB086550 and therapeutic antibodies share similar biological activities, there are critical differences. The mechanism of action of this class of small molecules is different from antibodies such as atezolizumab, which only block the PD-1–binding site on PD-L1. The increased potency of the small molecules when tumor cell expression of PD-L1 is high could allow lower doses to be effective. The ability to penetrate tumor tissue could be much improved for these molecules, providing options to treat previously refractory tumor histologies.

In summary, INCB086550 is established as a potent inhibitor of the PD-L1/PD-1 axis that possesses equivalent preclinical activity to clinically approved PD-L1 antibodies and has emerging clinical activity, which supports its ongoing investigation in patients. Therefore, small-molecule PD-L1 inhibitors may represent an important and effective alternative to restore antitumor immunity in patients with cancer.

METHODS

Reagents

INCB086550 was synthesized as a trifluoroacetic acid salt at Incyte Corporation. The compound was diluted in DMSO for the *in vitro* experiments. For *in vivo* studies, the compound was suspended in 5% dimethylacetamide in 0.5% (w/v) methylcellulose (Sigma, MC430) for oral dosing of BALB/c nu/nu mice. The 5% dimethylacetamide in 0.5% methylcellulose solution without INCB086550 was included in all studies as a control.

PD-1, PD-L1, and PD-L2 HTRF-Binding Assay

The assays were carried out at 25°C in phosphate-buffered saline (PBS) buffer (pH 7.4) with 0.05% Tween-20 and 0.1% BSA. Recombinant human, mouse, and cynomolgus proteins with His-tags were acquired from ACRO Biosystems and included human PD-L1 (PD1-H5229), human PD-L2 (PD2-H5220), mouse PD-L1 (PD1-M5220), cynomolgus PD-L1 (PD1-C52H4), and rat PD-L1 from

Sino Biological (80450-R08H). Recombinant human PD-1 protein with an Fc tag was also acquired from ACRO Biosystems (PD1-H5257). PD-L1 (L2) and PD-1 proteins were diluted in the assay buffer, and 10 μL was added to the plate well. Plate was centrifuged, and proteins were preincubated with inhibitor for 40 minutes. The incubation was followed by the addition of 10 μL of HTRF detection buffer supplemented with Europium cryptate-labeled anti-human IgG (PerkinElmer, AD0212) specific for Fc and anti-His antibody conjugated to SureLight Allophycocyanin (PerkinElmer, AD0059H). After centrifugation, the plate was incubated at 25°C for 60 minutes before reading on a PHERAstar FS plate reader (665 nm/620 nm ratio). Final concentrations in the assay were 3 nmol/L PD-1 and 10 nmol/L PD-L1 (human PD-1/human PD-L1 assay), 3 nmol/L PD-1 and 4 nmol/L PD-L2 (human PD-1/human PD-L2 assay), 5 nmol/L PD-1 and 20 nmol/L PD-L1 (human PD-1/mouse PD-L1 assay), 5 nmol/L PD-1 and 10 nmol/L PD-L1 (human PD-1/cynomolgus PD-L1 assay), 3 nmol/L PD-1 and 10 nmol/L PD-L1 (human PD-1/rat PD-L1 assay). Final concentrations of detection reagents in all assays were 1 nmol/L Europium anti-human IgG and 20 nmol/L anti-His allophycocyanin. The assays were conducted in standard black 384-well polystyrene plate in a final volume of 20 μL. Inhibitor was first serially diluted in DMSO and added to the plate wells before the addition of other reaction components. The final concentration of DMSO in the assay was 1%.

PD-1–SHP Reporter Assay

U2OS/PD-L1 and Jurkat-PD-1-SHP cells were first centrifuged in conical tube to remove the culture media, then washed and resuspended with assay medium (RPMI 1640 medium with 1% FBS) before cell plating. The U2OS/PD-L1 cells were first added in 384-well black clear-bottom assay plate (CELLCOAT Tissue Culture Plates, Greiner Bio-One) at 5,000 cells per well in 20 μL assay medium. INCB086550 was prepared by serial dilution in DMSO, and 125 nL compound was first transferred to the 384 REMP plate well (Thermo Fisher Scientific) by Echo liquid handler (Labcyte) followed by addition of 27.5 μL assay medium. INCB086550 (5 μL/well) was transferred to the cell plate with 0.05% DMSO in the final assay at 0.25 μmol/L and incubated at 37°C, 5% CO_2 for 1 hour. Jurkat-PD-1-SHP cells were added next to the cell plates at 5,000 cells per well in 20 μL assay medium and incubated at 37°C, 5% CO_2 for 2 hours before the addition of 2.5 μL PathHunter reagent 1 in each well. The assay plate was then shaken for 1 minute at 350 rpm and kept in the dark for 15 minutes at room temperature followed by addition of 10 μL PathHunter reagent 2. Chemiluminescent signal was recorded using a TopCount reader (PerkinElmer) after incubation at room temperature for 1 hour. Wells with DMSO were used as positive controls, and wells without any cells were used as negative controls. IC_{50} determination was performed by fitting the curve of percent control activity versus the log of the compound concentration using GraphPad Prism 6.0 software. U2OS/PD-L1 cells, Jurkat-PD-1-SHP cells, and PathHunter reagent 1 and 2 were purchased from DiscoverX Corporation. Puromycin, hygromycin B, G418, RPMI 1640 medium, and McCoy's 5A medium were purchased from Thermo Fisher Scientific. U2OS/PD-L1 cells were maintained in McCoy's 5A medium with addition of 10% FBS + 0.25 μg/mL puromycin. Jurkat-PD-1-SHP cells were cultured in RPMI 1640 medium supplemented with 10% FBS, 250 μg/mL hygromycin B, and 500 μg/mL G418.

NFAT Reporter Assay

PD-L1 artificial antigen-presenting cells (aAPC)/CHO-K1cells and Jurkat-PD-1-NFAT effector cells were centrifuged first to remove the culture media, and washed, resuspended with assay medium (RPMI 1640 medium with 1% FBS) before cell plating. The PD-L1 aAPC/CHO-K1 cells were added to a 384-well white clear-bottom assay plate (CELLCOAT Tissue Culture Plates, Greiner Bio-One) at 8,000

cells per well in 10 μL assay medium. INCB086550 was prepared by serial dilution in DMSO, and 0.8 μL of test article in DMSO was first transferred to the 384 REMP plate well (Thermo Fisher) by PlateMate Plus (Thermo Fisher) followed by addition of 50 μL plating medium. INCB086550 (5 μL/well) was transferred to the cells with 0.4% DMSO in the final assay at 2 μmol/L. Jurkat-PD-1-NFAT effector cells were dispensed into each well at 10,000 cells per well in 5 μL assay medium. The assay plate was incubated at 37°C, 5% CO_2 for 24 hours. After the assay plate was equilibrated to room temperature for 15 minutes, 20 μL/well of Bio-Glo reagent was added. After an 8-minute incubation at room temperature, luminescence was measured using the PHERAstar microplate reader (BMG Labtech). The fold of induction (FOI) was calculated based on the ratio of luminescence normalized to the DMSO wells within each assay plate. The maximum percentage of induction was reported based on the ratio between the highest FOI of each compound and the maximum FOI of control compound within each assay plate. Wells with DMSO served as the negative controls and wells containing control compound with the highest FOI were used as positive controls. EC_{50} determination was performed by fitting the curve of percent control activity versus the log of the compound concentration using the GraphPad Prism 6.0 software. PD-L1 aAPC/CHO-K1 cells, Jurkat-PD-1-NFAT effector cells and Bio-Glo reagent were purchased from Promega. Hygromycin B, geneticin (G418), RPMI 1640 medium, and F-12 medium were purchased from Thermo Fisher Scientific. PD-L1 aAPC/CHO-K1 cells were maintained in F-12 medium with addition of 10% FBS, 200 μg/mL hygromycin B, and 250 μg/mL geneticin (G418). Jurkat-PD-1-NFAT effector cells were cultured in RPMI 1640 medium supplemented with 10% FBS, 100 μg/mL hygromycin B, and 500 μg/mL G418.

Cell-Based PD-1 Binding Assay

PD-L1 aAPC/CHO-K1 cells ("CHO PD-L1"; Promega) were seeded at a density of 5,000 cells/well in 100 μL of F-12 medium (Gibco Laboratories) supplemented with 10% FBS (HyClone, GE Healthcare) into 96-well, high-content imaging plates (Greiner Bio-One) and incubated for 48 hours at 37°C. At the time of assay, the conditioned medium was removed and replaced with 50 μL F-12 medium containing 4% FBS. Cells were pretreated with 25 μL of INCB086550 for 15 minutes at room temperature, then 25 μL PE-labeled PD-1 (PD-1/PE, BPS Bioscience) was added to a final concentration of 400 nmol/L (8 μg/mL). Plates were incubated for 1 hour at 37°C. Cells were washed with PBS to remove unbound PD-1/PE, and fixed with 4% paraformaldehyde and nuclei stained with 1 μg/mL Hoechst 33342 for 10 minutes. Plates were scanned in the CellInsight CX5 high-content imager (Thermo Fisher) using 10 × magnification and the target activation protocol. Positively stained nuclei were used to identify valid cells, and the total intensity of fluorescence measured at 555 nm from the PE was measured. These intensity values were used to determine percentage inhibition, relative to the DMSO control, from which IC_{50} values were calculated using GraphPad Prism 8.2 software.

Blocking of PD-1 Binding to PD-L1 by INCB086550 by Flow Cytometry

CHO PD-L1 (Promega) or MDA-MB-231 cells were preincubated with 11 point 2.5 × dilution of INCB086550 starting at 1 μmol/L for 30 minutes at room temperature, 200 ng of PE-labeled PD-1 (BPS Bioscience, 7124301) was added per 200,000 cells (final concentration 2 μg/mL), and cells were incubated for an additional 20 minutes. Cells were washed, and levels of bound PD-1 PE were analyzed by flow cytometry (ACEA Biosciences, Agilent Technologies Inc.). Data were analyzed using NovoExpress software, and the percentage of inhibition was calculated using mean fluorescence intensity of the PE channel.

Size-Exclusion Chromatography: Multiangle Light Scattering

PD-L1 (aa 19–239) expressed in *Escherichia coli* (BPS, 100443) was exchanged into assay buffer (20 mmol/L phosphate buffer, 2.7 mmol/L KCl, 137 mmol/L NaCl, 0.05% Tween-20 at pH 7.4) using Zeba Spin Desalting Columns (Thermo Fisher, 7K MWCO, 0.5 mL). A 30-μL sample was made in assay buffer with 15 μmol/L of PD-L1 and 100 μmol/L of INCB086550 or peptide 71. Then 10 μL of the sample was loaded on an SEC multiangle light scattering instrument (Wyatt Technology) at a flow rate of 0.5 mL/minute on an ACQUITY UPLC Protein BEH SEC Column (Waters Corporation; particle size 1.7 μm, pore size 200 Å, diameter 2.1 mm, and length 150 mm). The elution was monitored using ultraviolet/visible trace at 280 nm. Approximate molecular weights of the eluted peaks were calculated using the MALS data (Wyatt QELS DLS, Wyatt Technology) and compared with apo PD-L1 with 2% DMSO.

Determination of Unoccupied and Total PD-L1 Following INCB086550 Treatment by Flow Cytometry

CHO PD-L1 or MDA-MB-231 cells were plated at 300,000 cells per well in a 6-well plate. The next day, cells were treated with varying concentrations of INCB086550 for 18 hours. Cells were harvested, washed with PBS, and stained separately with fluorescently labeled anti–PD-L1 clone MIH1 or anti–PD-L1 clone 28-8 for 30 minutes at room temperature. Samples were analyzed using flow cytometry (ACEA, Agilent), and data were analyzed by NovoExpress software. Percentage reduction was calculated using mean fluorescent intensity of each sample compared with untreated control.

Determination of Unoccupied PD-L1 on Monocytes in Whole Blood

To determine the effect of INCB086550 on monocyte surface PD-L1, 5 μL of the compound at appropriate dilutions was added to a 96-well assay block (Costar). Human IFNγ, (R&D Systems) at 1 ng/mL was added to whole blood from healthy donors, or SEB (Toxin Technologies Inc.) at 10 ng/mL was added to cynomolgus whole blood, and 95 μL of the mixture was then transferred to the assay block. A negative control with no stimulant was also included. Plates were incubated at 37°C in 5% CO_2 for 18 to 20 hours. Then, 5 μL of antibody mixture was added and incubated for 30 minutes in the dark. The Ab mixture for human whole blood samples consisted of 0.5 μL of anti-CD274 (clone MIH1, eBioscience; Thermo Fisher Scientific) + 0.5 μL of anti-CD14 (Life Technologies) + 4 μL staining buffer (0.5% BSA in PBS; BD Biosciences); the Ab mixture for cynomolgus whole blood samples consisted of 3 μL of anti-CD274 (clone MIHI, BD Biosciences, 557924) + 1 μL of anti-CD14 (Life Technologies, MHCD1405) + 1 μL CD11b (BioLegend, 301324). Prewarmed red blood cell lysis/fixation buffer (BD Biosciences) was added and incubated for 10 minutes at 37°C, plates were centrifuged at 1,600 rpm for 5 minutes, and 500 μL staining buffer was added to the pellet. Flow-cytometric analysis was performed. Cells were gated on CD14+ and read on PD-L1 mean fluorescence intensity (BD LSRFortessa X-20). The data were analyzed by FlowJo software and converted to percent inhibition relative to DMSO control, and IC_{50} determination was performed by fitting the curve of percent inhibition versus the log of the inhibitor concentration using GraphPad Prism 8.2 software.

Fluorescence Microscopy Studies

For confocal imaging of fixed cells, CHO PD-L1 cells were plated on CELLview glass-bottom slides (Greiner Bio-One; #543979) at 15,000 cells/well in 100 μL of growth medium. INCB086550 was added at a final concentration of 1 μmol/L after 24 hours, and cells were incubated at 37°C in a 5% CO_2 humidified atmosphere for an additional 16 hours. Control cells were treated with DMSO alone. After fixation

and permeabilization with an Image-iT Fixation/Permeabilization Kit (Thermo Fisher Scientific, R37602), cells were blocked with 0.5% BSA for 20 minutes at room temperature and incubated overnight at 4°C with primary recombinant anti-human PD-L1 antibody (clone 28-8) conjugated to Alexa Fluor 488 (Abcam, ab209959) diluted in blocking buffer at a 1:100 ratio. The cells were washed, and nuclei were counterstained with 4′,6-diamidino-2-phenylindole (DAPI). Images were taken using a 63× oil immersion objective on a Zeiss 880 confocal microscope.

For live-cell imaging, CHO PD-L1 cells were plated on CELLview glass-bottom slides (Greiner Bio-One, 543979) at 3,000 cells/well. After 24 hours, cells were stained with anti–PD-L1 clone 28-8 (Abcam, 209959) at 1:100 dilution for 1 hour at 4°C. Cells were washed three times with PBS, and phenol-free medium was added. Cells were incubated at 37°C in a 5% CO_2 environmental chamber, and INCB086550 was added to a final concentration of 1 μmol/L. Surface PD-L1 was monitored following the addition of INCB086550. Images were analyzed using Zen software (Zeiss).

For Golgi-colocalization studies, CHO PD-L1 cells were transduced with CellLight Golgi-RFP, BacMam 2.0, a fusion construct of human Golgi resident enzyme (N-acetylgalactosaminyltransferase) and TagRFP, packaged in the insect virus baculovirus. This approach provides accurate and specific targeting of RFP to the Golgi compartment. After positive transduction was verified, cells were subjected to treatment with INCB086550 (18 hours, 1 μmol/L), fixed and stained with anti–PD-L1 antibody conjugated to AlexaFluor-488. Nuclei were visualized with DAPI. Single-plane images were taken with a Zeiss 880 confocal microscope using 63× objective (oil immersion) and 1.8 × digital zoom.

PD-L1 Cell-Surface Recovery

MDA-MB-231 cells were treated with 250 nmol/L of INCB086550 for 18 hours. Residual compound was then washed from cell surface with acid wash (DMEM + 2% BSA, pH 3.6) and was set at time = 0 hours. Cells were harvested at designated time points, and levels of available PD-L1 were compared with untreated cells for each time point after staining with PD-L1 clone MIH1 antibody (eBioscience). Samples were run in triplicate, and percent of surface receptor was calculated using mean fluorescence intensity.

Isogenic Cell Line Studies

MBT2 isogenic cell lines were generated by genetically removing mouse PD-L1 using CRISPR-mediated genome editing technology. MBT2 PD-L1 knockout cells were generated and chimeric PD-L1 (mouse extracellular immunoglobulin domain was substituted with the human counterpart) was transfected into these cells. Following transfection, clones with different levels of chimeric PD-L1 expression were selected. To detect cell-surface PD-L1 after compound treatment, engineered MBT2 cells were seeded at 2×10^5 cells per well of a 6-well tissue culture plate in 2 mL of RPMI medium supplemented with 10% FBS allowed to attach for 24 hours. INCB086550 was diluted serially, resuspended with medium and transferred to each well; control wells received an equal volume of diluted DMSO (0.1% final). Cells were incubated in the presence of INCB086550 for 16 hours at 37°C in 5% CO_2. The cells were harvested, stained with anti-human CD274 antibody (clone M1H1), and analyzed by flow cytometry as described above.

Determination of Macrophage PD-L1 Internalization Induced by INCB086550

Malignant pleural effusion samples were obtained from patients with non–small cell lung cancer. The protocol received full approval by the University of Pennsylvania Medical Center Review Board. Written informed consent, in accordance with the Declaration of Helsinki protocols, was obtained from each patient at the time of enrollment. Patients were recruited and staged radiographically. Each patient then underwent a procedure to insert a tunneled intrapleural

catheter under local anesthesia as an outpatient. If this was not technically feasible, a pleural catheter was inserted via thoracoscopy under general anesthesia by thoracic surgery or via image-guided placement by interventional radiology.

Pleural effusion fluid samples were spun down to form cell pellet, followed by resuspending with AIM-V culture medium at the cell density of 5×10^6/mL; 10 μL of INCB086550 at appropriate dilutions were added to a 96-well assay block (Costar). Pleural effusion cells (190 μL) were then transferred to the assay block. In some studies, human IFNγ (R&D Systems) was added to the cell suspension to reach the final concentration of 1 ng/mL before the transfer. A negative control with no IFNγ was also included. Plates were incubated at 37°C in 5% CO_2 for 18–20 hours. Then, pleural effusion cells were washed with PBS and resuspended into BV 421 viability dye (BioLegend) solution. Plates were incubated at room temperature for 15 minutes in the dark. Then, cells were washed with PBS and resuspended in 50 μL PBS. Ab mixture (5 μL) was added and incubated for 30 minutes in the dark. The antibody mixture consisted of 3 μL of anti-CD274 (clone MIH1) + 0.5 μL of anti-CD14 (Life Technologies) + 1 μL of anti-CD11b (BD Biosciences). Prewarmed fixation buffer (BD Biosciences) was added and incubated for 10 minutes at 37°C, plates centrifuged at 1,600 rpm for 5 minutes and 500 μL staining buffer (BD Biosciences) was added to the pellet. Flow-cytometric analysis was performed. Cells were gated on CD14+ CD11b+ and read on PD-L1 mean fluorescence intensity (BD LSRFortessa X-20). The data were converted to percent inhibition relative to DMSO control and INCB086550. IC_{50} determination was performed by fitting the curve of percent inhibition versus the log of the inhibitor concentration using GraphPad Prism 6.0 software.

Artificial Antigen–Presenting Cell System

Mononuclear cells were isolated from leukopaks from normal donors using Ficoll gradient separation. T cells were enriched using the Pan T Cell Isolation Negative Selection Kit (Miltenyi Biotec) using the manufacturer's protocol. The isolated T cells were confirmed by anti-CD3 staining (>95% by flow cytometry) and frozen in CryoStor Freezing Media CS10 (BioLife Solutions) until use. Then 10^5 CHO PD-L1 cells were seeded into 96-well tissue culture plates in 100 μL of F-12 media with 10% FBS and allowed to attach overnight in a 37°C/5% CO_2 incubator. The next day, frozen T cells were thawed and resuspended to 1×10^6 cells/mL in T-cell medium (Iscove's modified Dulbecco's medium with 10% heat-inactivated FBS, 1 × glutamine, 1 × nonessential amino acid, 1,000 × mercaptoethanol, and 1 × sodium pyruvate). The media from the CHO PD-L1 cell plates were replaced with 130 μL of T-cell media. INCB086550 was serially diluted in DMSO and spotted into plates. The dots were resuspended in 100 × volume of T-cell media, and 20 μL of each compound was added to each well of the cell plate. Then, 50,000 T cells were transferred into each well and incubated at 37°C/5% CO_2 for 72 hours. After 3 days, the conditioned medium was harvested. The levels of hIFNγ and hIL-2 were assayed using a ProcartaPlex 2-plex kit (Thermo Fisher Scientific) for hIFNγ and hIL-2 according to the manufacturer's protocols and analyzed on a Luminex FLEXMAP 3D instrument. DMSO-treated cells were used as the control.

Staphylococcal Enterotoxin B Assay

To determine the effect of INCB086550 on enhancing SEB-stimulated cytokine release, 10 μL of diluted test drug, atezolizumab at appropriate dilutions or DMSO was added to a 96-well U-bottom tissue culture plate (Costar). Then 190 μL of whole blood from normal donors diluted 1/10 in AIM-V media (Gibco/Life Technologies) with 5 ng/mL of SEB (Toxin Technologies) or AIM-V only was then added to the plate and incubated at 37°C, 5% CO_2 for 72 hours. Plates were spun at 1,500 rpm for 10 minutes, and supernatants were harvested and tested for IFNγ levels by enzyme-linked immunosorbent assay (ELISA; R&D Systems, Human IFNγ Quantikine ELISA Kit). The data were converted to percent of control relative to DMSO + SEB. Atezolizumab was utilized as the assay control.

Pharmacokinetic Sample Analysis

Plasma and tumor concentrations of INCB086550 were determined with a calibration curve prepared in plasma. Tumor study samples were diluted 8- to 12-fold with water containing 0.1% formic acid and homogenized using the MPBio FastPrep-24 benchtop homogenizer. Plasma and tumor study sample aliquots (25 or 50 μL, respectively) were then deproteinized with vigorous mixing with at least five volumes of acetonitrile containing an internal standard (IS). After centrifugation, 100-μL samples of the supernatants were transferred to a 96-well plate containing 200 μL of water, mixed well, and analyzed by liquid chromatography–tandem mass spectrometry. Chromatography was performed using 0.5- to 2-μL injections of extracts with an ACE C18-AR (30 × 2.1 mm, 3 μmol/L, at 40°C) column under gradient conditions as described in Supplementary Table S2 at a flow rate of 0.75 mL/minutes. Then 0.1% formic acid in water and 0.1% formic acid in acetonitrile were used for mobile phase A and B, respectively. Liquid chromatography–tandem mass spectrometry analysis was performed using a Shimadzu Nexera ultra high-performance liquid chromatography system coupled to the electrospray ionization source (in positive ion mode) of a Sciex 6500+ triple quadrupole mass spectrometer. Peak areas for the multiple reaction monitoring transitions 694.1 > 365.1 for INCB086550 [retention time (RT) = 1.08 minutes] and 703.3 > 488.1 for the IS (RT = 1.13 minutes) were used to calculate analyte/IS peak area ratios, which were then used to create linear regression calibration equations with $1/x^2$ weighting. Sciex Analyst software (version 1.6.3) was used to acquire the raw data and to calculate calibration curves, and study sample concentrations. The assay range was adjusted for anticipated study concentrations, generally ranging from 0.5 to 2,000 nmol/L.

IHC

IHC was performed at Indivumed. Tumor samples were fixed in 4% neutral buffer formaldehyde solution (10% formalin) and transferred to 70% ethanol at Incyte Corporation. Subsequently, the formalin-fixed samples were embedded in paraffin at Indivumed according to Indivumed's standard operating procedure. IHC was implemented on the Discovery XT staining platform (Roche Diagnostics/Ventana Medical Systems), using the rabbit monoclonal anti–PD-L1 antibody clone SP142 (Spring BioScience/Ventana). Formalin-fixed, paraffin-embedded tissue samples were sliced into 3- to 5-μm sections and mounted on Superfrost Ultra Plus glass slides (Carl Roth). Sections were deparaffinized within the staining instrument and immunostained using the Discovery ChromoMap DAB Kit (Roche Diagnostics). After staining, the slides were manually washed using hot tap water supplemented with detergent, followed by tap water only and distilled water in a final step. For dehydration, the slides were transferred to an ascending ethanol series (2 × 80%, 2 × 96%, 2 × abs. EtOH; 1 minutes each). After dehydration, the slides were transferred to xylene (2 × 1 minutes) and automatically cover-slipped in Pertex mounting medium (International Medical Products). Scans were generated with the Axio Scan Z1 automated slide scanner (Zeiss) using ZEN 2 (blue edition) slide scan software (Zeiss).

Determination of Available and Total PD-L1 on Tumor Cells

Animal studies were conducted under the supervision of a veterinarian and in compliance with Incyte Corporation's Animal Use Protocols, established and approved by the Incyte Institutional Animal Care and Use Committee. Female BALB/c nu/nu mice (5–8 weeks of age; Charles River Laboratories) were inoculated subcutaneously with 3×10^6 MDA-MB-231 cells (ATCC# HTB-26). The treatment of tumor-bearing mice was started when tumor volume reached

approximately 250–400 mm³. INCB086550 was given at 15 and 200 mg/kg orally once or twice. Tumors were harvested 24 hours after initial dose and processed into single-cell suspension for flow cytometry analysis. To determine the pharmacokinetic profile of INCB086550 in plasma and tumors, mice bearing MDA-MB-231 xenografts were dosed with 150 mg/kg of INCB086550 orally. Animals were euthanized at various time points, and blood and tumors were collected to determine compound concentration. On harvesting, the tumors were cut into halves. One half was snap-frozen for pharmacokinetic sample analysis, and the other half was transferred into a 15-mL conical tube (Corning) containing 3 mL of RPMI 1640 medium with 10% fetal calf serum for flow-cytometric analysis.

Female C57BL/6 mice bearing MC38 hu-PD-L1 tumors approximately 100 mm³ in size were dosed with INCB086550 orally b.i.d. at 2, 20, or 200 mg/kg. After 14 days of dosing, tumors were collected 4 hours after the last dose and processed into single-cell suspension for flow-cytometric analyses (as described above) to determine the PD-L1 surface expression.

In Vivo *Efficacy Studies*

Animal studies were conducted under the supervision of a veterinarian and in compliance with Incyte Corporation's Animal Use Protocols, established and approved by the Incyte Institutional Animal Care and Use Committee. For the *in vivo* assessment of INCB086550, C57BL/6 or NSG mice (Charles River Laboratories) were inoculated subcutaneously with 1.25×10^6 human PD-L1–overexpressing murine MC38 colorectal cancer cells (Biocytogen LLC). When the tumors reached approximately 100–150 mm³, mice were randomly divided into groups (N = 8 per group). INCB086550 was given by oral gavage at doses of 2, 20, or 200 mg/kg b.i.d. until the end of the study. Mice were administered human IgG1 and atezolizumab at 5 mg/kg dosed intraperitoneally every 5 days. For the MDA-MB-231 tumor model, 3×10^6 MDA-MB-231 cells (ATCC# HTB-26) or MDA-MB-231 PD-L1 KO cells were inoculated with 50% Matrigel (BD, 354263) into 28-week-old female human CD34+ reconstituted NSG mice or 8- or 10-week-old female NSG mice (The Jackson Laboratory). MDA-MB-231 PD-L1 KO cells were generated using CRISPR technology. When tumors reached approximately 124 mm³, MDA-MB-231 tumor–bearing humanized mice were randomized by both tumor volume and donor followed by oral dosing with INCB086550 at 20, 60, or 200 mg/kg b.i.d. Mice in the study were engrafted with CD34+ stem cells from two donors. MDA-MB-231–inoculated NSG mice were randomized by tumor volume when tumors were approximately 163 mm³. Efficacy studies in the MDA-MB-231 model consisted of N = 10 mice per group. To generate HT-29 tumors, 3 million HT29 cells were inoculated into female CD34+ NOG mice (Taconic). Dosing was continuous throughout the studies. Tumor volume was calculated using the formula $(L \times W^2)/2$, where L and W refer to the length and width dimensions, respectively. Statistical significance for efficacy studies was determined using two-way analysis of variance with Dunnett multiple comparisons test using GraphPad Prism 8.2 software.

RNA-seq Analysis

RNA was isolated from cell-derived xenograft tumors and aligned to the human and mouse references using OmicSoft Array Studio software (Qiagen) with the human-aligned data being used for subsequent analysis. Mouse sequences were excluded, and only human gene expression was analyzed. Data from GSE91061 (21) were downloaded from the Gene Expression Omnibus hosted by the National Center for Biotechnology Information. Fragments per kilobase of transcript per million mapped reads of the data frame were then $\log_2$ transformed. Paired *t* test implemented in Array Studio was used to analyze the pre- and posttreatment data. The 58 genes were selected based on fold change >1.2 and raw *P* value < 0.05 in posttreatment samples compared with pretreatment samples. GO term enrichment

analysis was performed using the hypergeometric test implemented in the gprofiler2 R package with suitable background genes selected for each assay type (36). The g:SCS method was used to adjust *P* values for multiple testing, and the top-enriched Biological Process GO terms were identified.

Determination of Available PD-L1 on Monocytes from Clinical Study Patients

Whole blood was collected in sodium heparin tubes on cycle 1 day 3 predose and after a single dose of INCB086550 at 0.5, 1, 2, 3, 4, 6, 8, 24, and 48 hours. Additional samples were collected predose on cycle 1 day 1, day 8, and day 15. Samples were shipped ambient for testing; 95 µL of each heparinized blood sample was dispensed into a 96-well, 2-mL assay block. Aliquots of blood were left untreated or treated with 5.3 µL of 200 ng/mL human IFNγ (10 ng/mL final concentration), 5 µL DMSO (final concentration 0.1%), or 5 µL of 100 µmol/L INCB086550 (5 µmol/L final concentration). Samples were incubated for 19 hours at 37°C in 5% CO_2. For antibody staining, a 5-µL cocktail containing 0.5 µL of anti–PD-L1 (clone MIH1; BD Biosciences), 0.5 µL of anti-CD14 (Life Technologies), and 4 µL staining buffer (0.5% BSA in PBS; BD Biosciences) was added to the samples and incubated for 30 minutes in the dark. Prewarmed red blood cell lysis/fixation buffer (BD Biosciences) was then added and incubated for an additional 10 minutes at 37°C. Plates were then centrifuged at $569 \times g$ (1,600 rpm) for 5 minutes, supernatant was removed, and pellets were resuspended with 400 µL staining buffer, and then 200 µL of sample was transferred to a 96-well U-bottom plate (BD Falcon 353910) for analysis by flow cytometry on the FACSLyric. Cells were gated for CD14+ and then analyzed for PD-L1 (gMFI) expression, eliminating values outside of validated assay criteria of 500 ± 100 events.

Data were initially analyzed using FACSuite software (BD Biosciences-EU) for each subject and subsequently analyzed with a FlowJo template that was applied to all samples in the INCB86550-102 study to ensure consistency. The data were converted to percent inhibition relative to the DMSO control calculated by an SAS (Statistical Analysis System) program. The PD-L1 percent inhibition was correlated with the plasma concentration of INCB086550 obtained from PK samples collected in concert with the PD samples. An IC_{50} determination was performed by fitting the curve of percent inhibition of PD-L1 versus the log of the plasma concentration using GraphPad Prism 8.2 software.

Measurement of Proteins in Peripheral Blood

Plasma was prepared from sodium heparin blood collected before treatment, at cycle 1 day 8, and at cycle 2 day 1 from 18 patients in the clinical study. The plasma was frozen and shipped for analysis by immunoassays. CXCL9, CXCL10, and PD-L1 were measured using the ProteinSimple Ella immunoassay platform (Biotechne) following the manufacturer's instructions. IFNγ was assessed by the MSD assay platform (Meso Scale Diagnostics) following the manufacturer's instructions. In addition, plasma samples were assessed on a panel of 1,104 analytes utilizing the Olink proximity extension assay platform (Olink Proteomics).

Isothermal Titration Calorimetry

PD-L1 (aa 19-239) expressed in *E. coli* (BPS, 100443) was exchanged into assay buffer (20 mmol/L phosphate buffer, 2.7 mmol/L KCl, 137 mmol/L NaCl, 0.05 Tween-20 at pH 7.4) using Zeba Spin Desalting Columns (Thermo Fisher 7K MWCO, 0.5 mL). Protein and compound solutions were degassed at room temperature before analysis. Then 200 µL of 50 µmol/L solution of INCB086550 were prepared in buffer (20 mmol/L phosphate buffer, 2.7 mmol/L KCl, 137 mmol/L NaCl, 0.05 Tween-20 at pH 7.4) to a final DMSO concentration of 1%. Compound was titrated into 300 µL of 10 µmol/L PD-L1 (cell volume 185 µL) in 1% DMSO. All measurements were conducted at room

temperature on an Affinity ITC Low Volume (TA Instruments). Titrations included 22–30 × 1.5 μL injections of compound, with 120 seconds spacing between each injection, and stirred at 75 rpm throughout the experiment. Blank titration included 30 × 1.5 μL injection of ITC buffer with 1% DMSO. Data were then analyzed using NanoAnalyze software (TA Instruments) and fit using the Independent model.

SPR Antibody Competition Experiments

All experiments were performed on Biacore S200 (GE Healthcare, currently Cytiva) at 25°C. Biacore chips, reagents and buffers were from GE Healthcare. Atezolizumab (Selleckchem, A2004) and durvalumab (Selleckchem, A2013) were immobilized on CM5 chip using standard amine coupling with HBS-P$^+$ buffer (10 mmol/L HEPES, 150 mmol/L NaCl, 0.05% surfactant P20, pH 7.4) as a running buffer. The surface of flow cells was activated using the mixture of 0.1 M NHS (N-hydroxysuccinimide) and 0.4 M EDC (1-ethyl-3-(3-dimethylaminopropyl)-carbodiimide hydrochloride) at 1:1 ratio for 7 minutes at 10 μL/minute. Atezolizumab and durvalumab were diluted in acetate buffer, pH 5.5 to 10 μg/mL and 5 μg/mL, respectively. The specified level of attachment was reached at 500 RU. The residual activated groups were blocked by the injection of 1 M ethanolamine HCl, pH 8.5 for 7 minutes. Human PD-L1-FLAG tag protein (BPS Bioscience, 71183) was diluted in PBS-P$^+$ buffer with 1% DMSO to final concentrations of 8.1, 2.7, 0.9, 0.3, and 0.1 nmol/L. Similar PD-L1 dilutions were made in buffer with 1 μmol/L INCB086550. A-B-A injection was used to perform SPR competition assay at 50 μL/minute flow rate, 90-second injection and 310-second dissociations. Then 10 mmol/L glycine, pH 1.5, was used for surface regeneration at flow rate of 30 μL/minute for 30 seconds. A solvent correction cycle was included in the run. The sensorgrams were analyzed with BiacoreS200 Evaluation software. After solvent correction and double referencing for a blank reference cell and zero compound concentration (buffer injections), the curve was fit to 1:1 binding model.

Data Availability

The data generated in this study are available within the article and its supplementary data files.

Acknowledgments

REFERENCES

1. Postow MA, Callahan MK, Wolchok JD. Immune checkpoint blockade in cancer therapy. J Clin Oncol 2015;33:1974–82.
2. Akinleye A, Rasool Z. Immune checkpoint inhibitors of PD-L1 as cancer therapeutics. J Hematol Oncol 2019;12:92.
3. Beatty GL, Gladney WL. Immune escape mechanisms as a guide for cancer immunotherapy. Clin Cancer Res 2015;21:687–92.
4. Ribas A, Wolchok JD. Cancer immunotherapy using checkpoint blockade. Science 2018;359:1350–5.
5. Powles T, Eder JP, Fine GD, Braiteh FS, Loriot Y, Cruz C, et al. MPDL3280A (anti-PD-L1) treatment leads to clinical activity in metastatic bladder cancer. Nature 2014;515:558–62.
6. Iwai Y, Ishida M, Tanaka Y, Okazaki T, Honjo T, Minato N. Involvement of PD-L1 on tumor cells in the escape from host immune system and tumor immunotherapy by PD-L1 blockade. Proc Nat Acad Sci U S A 2002;99:12293–7.
7. Okudaira K, Hokari R, Tsuzuki Y, Okada Y, Komoto S, Watanabe C, et al. Blockade of B7-H1 or B7-DC induces an anti-tumor effect in a mouse pancreatic cancer model. Int J Oncol 2009;35:741–9.
8. Zhou Q, Xiao H, Liu Y, Peng Y, Hong Y, Yagita H, et al. Blockade of programmed death-1 pathway rescues the effector function of tumor-infiltrating T cells and enhances the antitumor efficacy of lentivector immunization. J Immunol 2010;185:5082–92.
9. Blank C, Kuball J, Voelkl S, Wiendl H, Becker B, Walter B, et al. Blockade of PD-L1 (B7-H1) augments human tumor-specific T cell responses in vitro. Int J Cancer 2006;119:317–27.
10. Skalniak L, Zak KM, Guzik K, Magiera K, Musielak B, Pachota M, et al. Small-molecule inhibitors of PD-1/PD-L1 immune checkpoint alleviate the PD-L1-induced exhaustion of T-cells. Oncotarget 2017;8:72167–81.
11. Zhan MM, Hu XQ, Liu XX, Ruan BF, Xu J, Liao C. From monoclonal antibodies to small molecules: the development of inhibitors targeting the PD-1/PD-L1 pathway. Drug Discov Today 2016;21:1027–36.
12. Guzik K, Tomala M, Muszak D, Konieczny M, Hec A, Blaszkiewicz U, et al. Development of the inhibitors that target the PD-1/PD-L1 interaction-a brief look at progress on small molecules, peptides and macrocycles. Molecules 2019;24:2071.
13. Magiera-Mularz K, Kocik J, Musielak B, Plewka J, Sala D, Machula M, et al. Human and mouse PD-L1: similar molecular structure, but different druggability profiles. iScience 2021;24:101960.
14. Miller MM, Mapelli C, Allen MP, Bowsher MS, Boy MK, Gillis EP, et al.; Bristol-Myers Squibb Company, assignee. Macrocyclic inhibitors of the PD-1/PD-L1 and CD80(B7-1)/PD-L1 protein/protein interactions. US patent WO2014151634. 2014.
15. Magiera-Mularz K, Skalniak L, Zak KM, Musielak B, Rudzinska-Szostak E, Berlicki Ł, et al. Bioactive macrocyclic inhibitors of the PD-1/PD-L1 immune checkpoint. Angew Chem Int Ed Engl 2017;56: 13732–5.
16. Perry E, Mills JJ, Zhao B, Wang F, Sun Q, Christov PP, et al. Fragment-based screening of programmed death ligand 1 (PD-L1). Bioorg Med Chem Lett 2019;29:786–90.
17. Huang A, Peng D, Guo H, Ben Y, Zuo X, Wu F, et al. A human programmed death-ligand 1-expressing mouse tumor model for evaluating the therapeutic efficacy of anti-human PD-L1 antibodies. Sci Rep 2017;7:42687.
18. Gao Y, Nihira NT, Bu X, Chu C, Zhang J, Kolodziejczyk A, et al. Acetylation-dependent regulation of PD-L1 nuclear translocation dictates the efficacy of anti–PD-1 immunotherapy. Nat Cell Biol 2020;22:1064–75.
19. Sharpe AH, Wherry EJ, Ahmed R, Freeman GJ. The function of programmed cell death 1 and its ligands in regulating autoimmunity and infection. Nat Immunol 2007;8:239–45.
20. Rios-Doria J, Stevens C, Maddage C, Lasky K, Koblish HK. Characterization of human cancer xenografts in humanized mice. J Immunother Cancer 2020;8:e000416.
21. Riaz N, Havel JJ, Makarov V, Desrichard A, Urba WJ, Sims JS, et al. Tumor and microenvironment evolution during immunotherapy with nivolumab. Cell 2017;171:934–49.
22. Abu Hejleh T, Furqan M, Ballas Z, Clamon G. The clinical significance of soluble PD-1 and PD-L1 in lung cancer. Crit Rev Oncol Hematol 2019;143:148–52.
23. Gorbachev AV, Kobayashi H, Kudo D, Tannenbaum CS, Finke JH, Shu S, et al. CXC chemokine ligand 9/monokine induced by IFN-gamma production by tumor cells is critical for T cell-mediated suppression of cutaneous tumors. J Immunol 2007;178:2278–86.
24. Liu M, Guo S, Stiles JK. The emerging role of CXCL10 in cancer (review). Oncol Lett 2011;2:583–9.
25. Iwai Y, Hamanishi J, Chamoto K, Honjo T. Cancer immunotherapies targeting the PD-1 signaling pathway. J Biomed Sci 2017;24:26.
26. Pillai RN, Behera M, Owonikoko TK, Kamphorst AO, Pakkala S, Belani CP, et al. Comparison of the toxicity profile of PD-1 versus PD-L1 inhibitors in non-small cell lung cancer: a systematic analysis of the literature. Cancer 2018;124:271–7.
27. Conner KP, Devanaboyina SC, Thomas VA, Rock DA. The biodistribution of therapeutic proteins: mechanism, implications for pharmacokinetics, and methods of evaluation. Pharmacol Ther 2020;212:107574.
28. Acurcio RC, Scomparin A, Conniot J, Salvador JAR, Satchi-Fainaro R, Florindo HF, et al. Structure-function analysis of immune checkpoint receptors to guide emerging anticancer immunotherapy. J Med Chem 2018;61:10957–75.
29. Park JJ, Thi EP, Carpio VH, Bi Y, Cole AG, Dorsey BD, et al. Checkpoint inhibition through small molecule-induced internalization of programmed death-ligand 1. Nat Commun 2021;12:1222.
30. Pardoll DM. The blockade of immune checkpoints in cancer immunotherapy. Nat Rev Cancer 2012;12:252–64.
31. Jiang X, Wang J, Deng X, Xiong F, Ge J, Xiang B, et al. Role of the tumor microenvironment in PD-L1/PD-1-mediated tumor immune escape. Mol Cancer 2019;18:10.
32. Ayers M, Lunceford J, Nebozhyn M, Murphy E, Loboda A, Kaufman DR, et al. IFN-gamma-related mRNA profile predicts clinical response to PD-1 blockade. J Clin Invest 2017;127:2930–40.
33. Zhou J, Mahoney KM, Giobbie-Hurder A, Zhao F, Lee S, Liao X, et al. Soluble PD-L1 as a biomarker in malignant melanoma treated with checkpoint blockade. Cancer Immunol Res 2017;5:480–92.
34. Tumeh PC, Harview CL, Yearley JH, Shintaku IP, Taylor EJM, Robert L, et al. PD-1 blockade induces responses by inhibiting adaptive immune resistance. Nature 2014;515:568–71.
35. Herbst RS, Soria J-C, Kowanetz M, Fine GD, Hamid O, Gordon MS, et al. Predictive correlates of response to the anti-PD-L1 antibody MPDL3280A in cancer patients. Nature 2014;515:563–7.
36. Kolberg L, Raudvere U, Kuzmin I, Vilo J, Peterson H. gprofiler2 – an R package for gene list functional enrichment analysis and namespace conversion toolset g:Profiler. F1000Res 2020;9:ELIXIR-709.